

N85-12931-

The
Allied
Bendix
Corporation

Guidance
Systems
Division

Teterboro
New Jersey 07608

AUTONOMOUS
MOMENTUM
MANAGEMENT
FOR
SPACE STATION

Final Report
15 October 1984

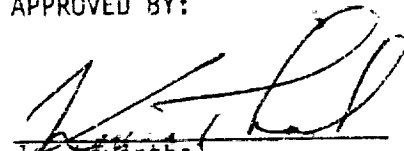
Prepared For:

George C. Marshall
Space Flight Center
Huntsville, Alabama

NASA Contract No.
NAS8-35349
Exhibit A

October 1, 1983
to
August 31, 1984

APPROVED BY:


J. Levinthal
Engineering Manager
Systems Design

PREPARED BY:

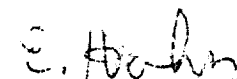

E. Hahn
Technical Manager

TABLE OF CONTENTS

<u>SECTION NO.</u>	<u>DESCRIPTION</u>	<u>PAGE</u>
	Foreword.....	iv
	Abstract.....	1
	Nomenclature.....	2
1.0	Introduction.....	5
2.0	Description of External Torques.....	7
3.0	Techniques Considered.....	20
4.0	Gravity Gradient Desaturation Using the Core Body.....	22
5.0	Aerodynamic Desaturation Using Flat Plate Appendages.....	35
6.0	Conclusions and Recommendations.....	62
7.0	References.....	64

LIST OF ILLUSTRATIONS

<u>FIGURE NO.</u>	<u>DESCRIPTION</u>	<u>PAGE</u>
1	CDG PLANAR SPACE STATION.....	6
2	AERO TORQUE, CORE BODY.....	9
3	GG TORQUE, CORE BODY.....	10
4	ATMOSPHERIC DENSITY IN ORBIT.....	11
5	AERO TORQUE, SOLAR ARRAY #1.....	12
6	GG TORQUE, SOLAR ARRAY #1.....	13
7	AERO TORQUE, FOUR SOLAR ARRAYS	14
8	GG TORQUE, FOUR SOLAR ARRAYS	15
9	AERO TORQUE, TOTAL VEHICLE.....	16
10	GG TORQUE, TOTAL VEHICLE.....	17
11	TOTAL TORQUE, TOTAL VEHICLE.....	18
12	MOMENTUM WITH NO MOMENTUM MANAGEMENT.....	19
13	CDG PLANAR SPACE STATION WITH AERODYNAMIC DESATURATION APPENDAGES.....	21
14	CORE BODY ANGLE ABOUT POP AXIS.....	23
15	POP MOMENTUM WITH CONTINUOUS CORE BODY CONTROL.....	24
16	IOP MOMENTUM WITH CONTINUOUS CORE BODY CONTROL.....	27
17	TILT PROFILE FOR CONTINUOUS IOP DESATURATION.....	28
18	TILT PROFILE FOR SINGLE ORBIT DESATURATION, RATE LIMIT = .01 DEG/SEC.....	30
19	IOP MOMENTUM WITH SINGLE ORBIT CORE BODY CONTROL.....	32
20	POP MOMENTUM WITH SINGLE ORBIT CORE BODY CONTROL.....	34
21	IOP DESATURATION APPENDAGES.....	38
22	IOP APPENDAGE TORQUE IN VEHICLE SPACE.....	41
23	DESIRED AND PERPENDICULAR IOP APPENDAGE TORQUE.....	42
24	OI X AND Z APPENDAGE TORQUE.....	43

LIST OF ILLUSTRATIONS (CONTINUED)

<u>FIGURE NO.</u>	<u>DESCRIPTION</u>	<u>PAGE</u>
25	IOP MOMENTUM, NO APPENDAGE CONTROL, RHOAVG = 1.7E-12, BETA = -45.....	44
26	IOP MOMENTUM, NO APPENDAGE CONTROL, RHOAVG = .34E-12, BETA = -45.....	45
27	IOP MOMENTUM, NO APPENDAGE CONTROL, RHOAVG = 8.5E-12, BETA = -45.....	46
28	IOP MOMENTUM, APPENDAGE CONTROL, TRIMMED CORE, RHOAVG = 1.7E-12, RHOCNTRL = 1.7E-12, BETA = -45.....	47
29	IOP MOMENTUM, APPENDAGE CONTROL, TRIMMED CORE, RHOAVG = .34E-12, RHOCNTRL = .34E-12, BETA = -45.....	48
30	IOP MOMENTUM, APPENDAGE CONTROL, TRIMMED CORE, RHOAVG = 8.5E-12, RHOCNTRL = 8.5E-12, BETA = -45.....	49
31	IOP MOMENTUM, APPENDAGE CONTROL, TRIMMED CORE, RHOAVG = .34E-12, RHOCNTRL = .34E-12, BETA = 0.....	51
32	IOP MOMENTUM, APPENDAGE CONTROL, RHOAVG = 8.5E-12, RHOCNTRL = 1.7E-12, BETA = -45.....	52
33	POP AXIS TORQUE EQUILIBRIUM ATTITUDE AS A FUNCTION OF AVERAGE DENSITY.....	53
34	POP APPENDAGE TORQUE.....	54
35	POP MOMENTUM, NO APPENDAGE CONTROL, TRIMMED CORE, RHOAVG = 1.7E-12.....	55
36	POP MOMENTUM, NO APPENDAGE CONTROL, TRIMMED CORE, RHOAVG = .34E-12, RHOCNTRL = .34E-12, BETA = -45.....	56
37	POP MOMENTUM, NO APPENDAGE CONTROL, TRIMMED CORE, RHOAVG = 1.7E-12.....	57
38	POP MOMENTUM, APPENDAGE CONTROL, TRIMMED CORE, RHOAVG = 1.7E-12, RHOCNTRL = 1.7E-12, BETA = -45.....	58
39	POP MOMENTUM, APPENDAGE CONTROL, TRIMMED CORE, RHOAVG = .34E-12.....	59
40	IOP MOMENTUM, APPENDAGE CONTROL, TRIMMED CORE, RHOAVG = 8.5E-12, RHOCNTRL = 8.5E-12, BETA = -45.....	60
41	POP MOMENTUM, APPENDAGE CONTROL, TRIMMED CORE, RHOAVG = 8.5E-12, RHOCNTRL = 1.7E-12, BETA = -45.....	61

Foreword

This final report is submitted in accordance with "Scope of Work, Exhibit D" for contract NAS8-35349. This study was directed from the Guidance Systems Division (GSD) of the Allied Bendix Aerospace Corporation. Mr. Eric Hahn was study manager and he appreciates the valuable guidance of Ms. Miriam Hopkins of The Marshall Space Flight Center (MSFC) who was the contracting officer. Additional important suggestions were made by Mr. Harry Buchanan and Mr. Stan Carroll of MSFC, Mr. Dave Barrows of McDonnell Douglas Astronautics Company and Mr. Ray Kaczynski of GSD.

Abstract

The report discusses momentum management for the CDG Planar Space Platform. The external torques on the Space Station are assumed to be gravity gradient and aerodynamic with both having bias and cyclic terms. The integrals of the cyclic torques are the cyclic momenta which will be stored in the momentum storage actuator. Various techniques to counteract the bias torques and center the cyclic momentum were investigated including gravity gradient desaturation by adjusting vehicle attitude, aerodynamic desaturation using solar panels and radiators and the deployment of flat plates at the end of long booms generating aerodynamic torques.

Nomenclature

A_p	transformation from p-th appendage principal axis to core body frame
cm	center of mass
C_d	drag coefficient (assumed = 2)
CMG	control moment gyro
cp	center of pressure
GG	gravity gradient
\underline{H}	instantaneous stored momentum
\overline{H}	estimated average angular momentum
I	identity matrix
IOP	in-orbit plane
I_p	inertia of p-th appendage
I_{pcm}	inertia of p-th appendage in cm coordinates
I_V	total vehicle inertia tensor
K_{db}	atmosphere diurnal bulge
LV	local vertical
m_p	mass of p-th appendage
\hat{N}	unit normal to p-th appendage
N-m	newton meters
N-m-s	newton meters seconds
OI	orbit inertial
POP	perpendicular to orbit plane
\hat{R}	unit radius vector from center of earth to center of mass
S	surface area of p-th flat plate
T_{By}	desired y-axis torque for bias counteraction
\underline{T}_D	desired control torque
\overline{T}_D	average value of IOP torque in desired direction

Nomenclature (Continued)

T_{DIOP}	desired control torque magnitude in orbit plane
T_{GG}	gravity gradient torque
T_{Iy}	desired y-axis centering torque
T_{nom}	nominal torque from one appendage if $\rho = \rho_{nom}$ and air flow is perpendicular to surface
T_o	orbital period
\bar{T}_{pa}	aerodynamic torque due to p-th appendage
\bar{T}_{\perp}	average value of IOP torque perpendicular to desired direction
U	vehicle angle from orbital noon
U_{db}	peak atmospheric density phase lag
U_{on}	half angle that IOP aerodynamic desaturation is "ON"
U_T	angle of desired torque IOP with orbital noon
V	velocity magnitude
\hat{v}	unit vector along relative wind
x_p	moment arm of p-th appendage
z	z-transform variable
ΔI_i	inertia difference ($\Delta I_i = I_k - I_j$, i, j, k in even permutation)
$\Delta \phi_1$	Δ -rotation of vehicle about POP axis to remove bias
$\Delta \phi_2$	Δ -rotation of vehicle about POP axis to center momentum
α	angle at panel "ON" makes with air flow for POP desaturation
β	angle of sunline to orbit plane
γ	angle of "ON" POP desaturation panel with air flow
ϕ	angle of vehicle z-axis to local vertical about POP axis
ϕ_p	angle of vehicle principal z-axis to local vertical about POP axis
ω_o	vehicle angular rate in orbit
π	3.1416

Nomenclature (Continued)

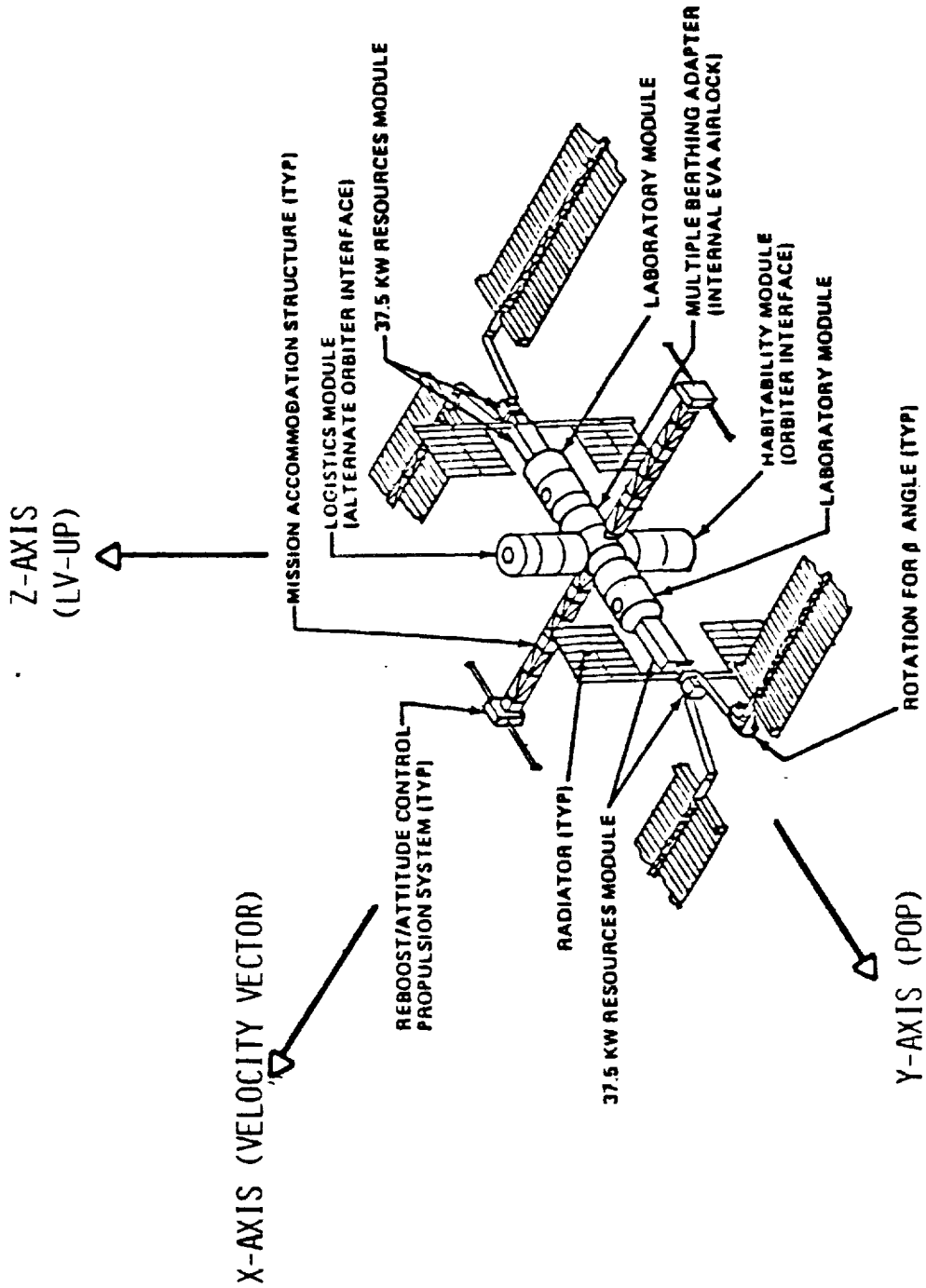
ρ	instantaneous atmospheric density
ρ_{avg}	average atmospheric density
ρ_{est}	estimated average atmospheric density
ρ_{nom}	nominal atmospheric density
θ	vehicle x-axis rotation for GG desaturation
θ'	maximum θ adjusted for finite maneuvering rate
$\dot{\theta}_{max}$	max rate for maneuvering vehicle about its x-axis

1.0 Introduction

Figure 1 represents the CDG planar space station configuration whose basic attitude has the Z-axis local vertical (LV), the Y-axis perpendicular to the orbit plane (POP) and the X-axis along the velocity vector. The solar arrays are maintained nominally perpendicular to the sunline requiring two degrees of freedom, one for the vehicle rotation and the second for the sunline with respect to the orbital plane (β -angle). The radiators are maintained POP and only edgewise illuminated by the sunline. However, unlike the solar arrays which have unlimited rotation capability, due to the necessity of fluid transfer between the space station and the radiators and the limited freedom of the plumbing interface, the radiators must be unwound during the dark side of the orbit.

If the balanced vehicle defined in Figure 1 were ideal, the principal axes of the core body would be perpendicular to the orbit plane and along local vertical and no gravity gradient torques due to core body would exist. The center of mass would be at the geometric center and no aerodynamic torques would exist. The only remaining torques would be a bias torque about the X-axis due to the non-zero β -angle of the solar arrays and a cyclic torque about the POP axis due to the solar arrays. The radiators only contribute torque during the unwind cycle and were determined not to be significant for sizing momentum storage and desaturation requirements. For the actual inertias and center of mass used for the study, significant core body gravity gradient biases and aerodynamic torques do exist although the balanced design insures their being of small magnitude for the size of the vehicle investigated. The momentum storage system assumed for this study was four Skylab type double gimbal control moment gyros (CMGs) having an angular momentum of 3000 N-m-s each.

The main effort of this study was to develop momentum management techniques to counteract the bias torques and also to center the stored cyclic momentum along three inertial axes. Prior to developing momentum management techniques, it was necessary to define disturbance torques for the basic vehicle. Two types of disturbance torques were admitted for this study; gravity gradient and aerodynamic. Gravity gradient torques were defined by



CDG PLANAR SPACE STATION

FIGURE 1 CDG PLANAR SPACE STATION

the standard equations while aerodynamic torques were defined by a combination of flat-plate areas, a simple orbital curve fit to the Jacchia density model and inelastic collision of particles with the flat plates. The definition of torques is complicated by the relative motion of the appendages with respect to the core body leading to the selection of seven independent bodies to represent the total inertia. These bodies are the core, four solar arrays and two radiator sets. Nominally, the four solar arrays and two radiator sets each move as units but separate motions were allowed in order to investigate their use as desaturation techniques.

2.0 Description of External Torques

The inertia of the entire vehicle is defined as that of the core body plus the inertias of the appendages reflected to the center of mass of the system. Due to their symmetric nature, the center of mass of the solar arrays and the radiators are at the center of symmetry of the core body. However the center of mass (cm) of the core body is slightly offset from the center of symmetry. The inertia of an appendage relative to the cm of the core body consists of the sum of the inertia due to its own inertia matrix about its cm and the inertia moment of a point mass at the appendage cm acting about the core body cm. The appendage inertia must be transformed via a similarity transform from its principal axes to the axes fixed in the core body. The transformation varies with appendage attitude. The variable inertia due to an appendage is defined by equation 1 while the gravity gradient torque is defined by equation 2. The gravity gradient torque on the total vehicle can be defined two ways of which the first is the gravity gradient torque due to the total inertia of the core body and appendages. The second is to define the inertia of each appendage, determine the gravity gradient torque and add the individual torques to generate the total gravity gradient torque. The latter approach allows one to see the contribution of the individual appendages for insight into possible desaturation techniques. The aerodynamic torque due to the core body and each appendage is simply the force on each body and a vector cross product of that force with the vector between the cm and the center of pressure (cp). This torque is defined by equation 3.

$$\underline{I}_{pcm} = A_p \underline{I}_p A_p^T + m_p (\underline{X}_p^T \underline{X}_p \underline{I} - \underline{I} \underline{X}_p \underline{X}_p^T) \quad (1)$$

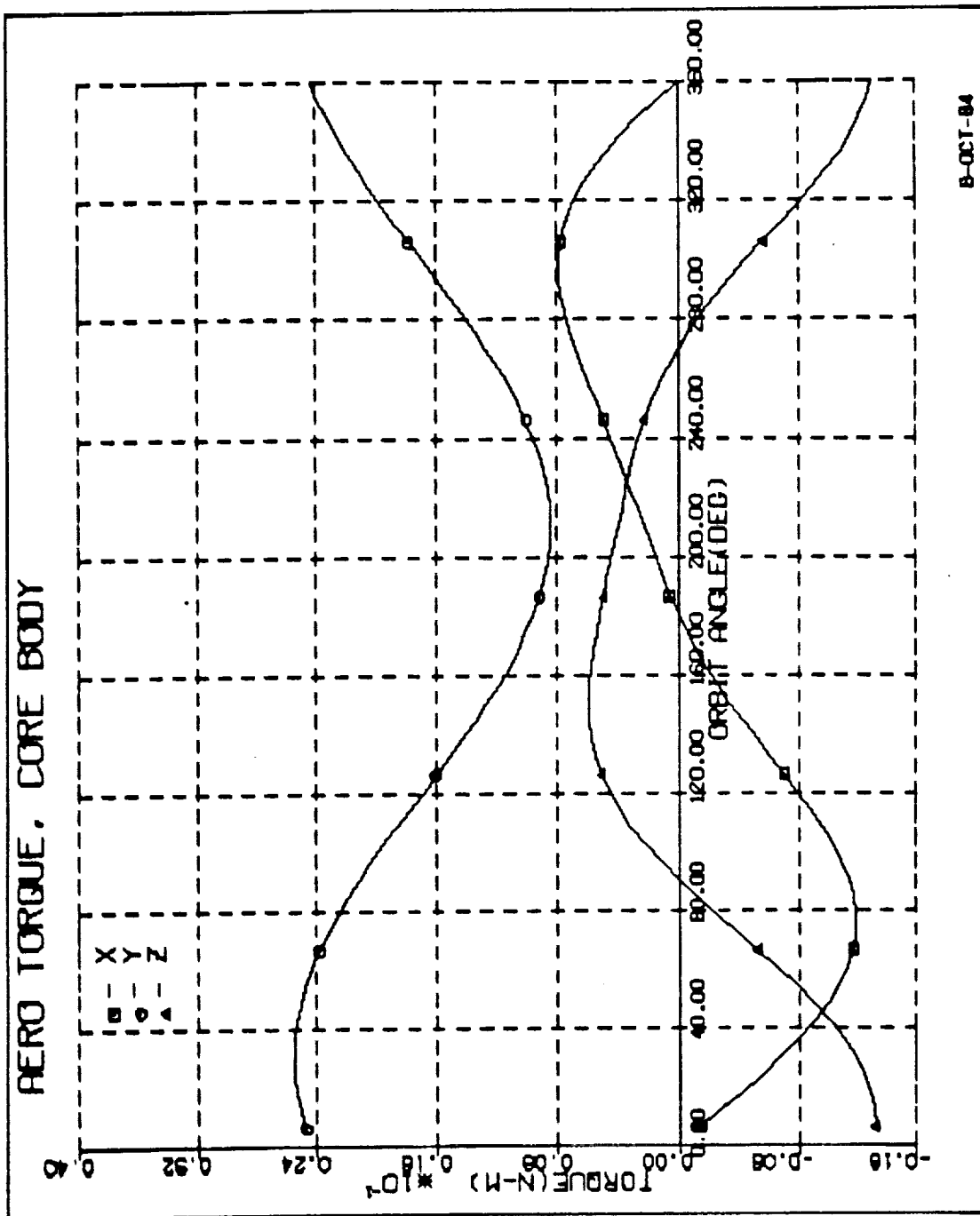
$$\underline{I}_{GG} = 3\omega_0^2 (\underline{R} \times \underline{I}_V \underline{R}) \quad (2)$$

$$\underline{I}_{pa} = \underline{X}_p \times (\frac{1}{2}\rho V^2) C_D S_p \underline{\hat{V}} \cdot \underline{\hat{R}}_p \underline{\hat{V}} \quad (3)$$

The flat plate area of the core is defined as the projection of a cylinder onto a plane. Figure 2 shows the aero torques due to the core body. The torque perpendicular to the orbit plane (POP) is in the same direction and only varies in magnitude due to the diurnal bulge. The torques in the orbit plane (IOP) are essentially cyclic but have bias components due to the diurnal bulge. The gravity gradient (GG) POP torque shown in Figure 3 is a bias while the IOP torques are cyclic in Orbit Inertial (OI) space. All IOP torques and momenta will be displayed in OI rather than body axis as that is the frame where momentum buildup truly occurs and in which it must be desaturated. The density variation in an orbit is given by equation 4, a simple curve fit to the Jacchia model of the nominal atmosphere.

$$\rho = \rho_{avg} (1 + K_{DB} \cos(U - U_{DB})) \quad (4)$$

Figure 4 shows a typical density variation over an orbit with the peak density occurring 30 degrees after noon and the minimum density occurring 30 degrees after midnight. Figure 5 shows the aero torque due to a single solar array with significant torques on all axes which is the same condition observed for the GG torques of Figure 6. Figure 7 shows that the aerodynamic torque due to four solar arrays is much less as the majority of the moment arms cancel. If the cm of the core body were at the center of symmetry, no solar array aero torques would exist. The cyclic gravity gradient torques due to the individual panels cancel IOP but add POP. Figures 8, 9, 10 and 11 show that the total torques on the vehicle are dominated by the solar arrays. However the dominant bias component POP is the GG torque



B-OCT-84

FIGURE 2 AERO TORQUE, CORE BODY

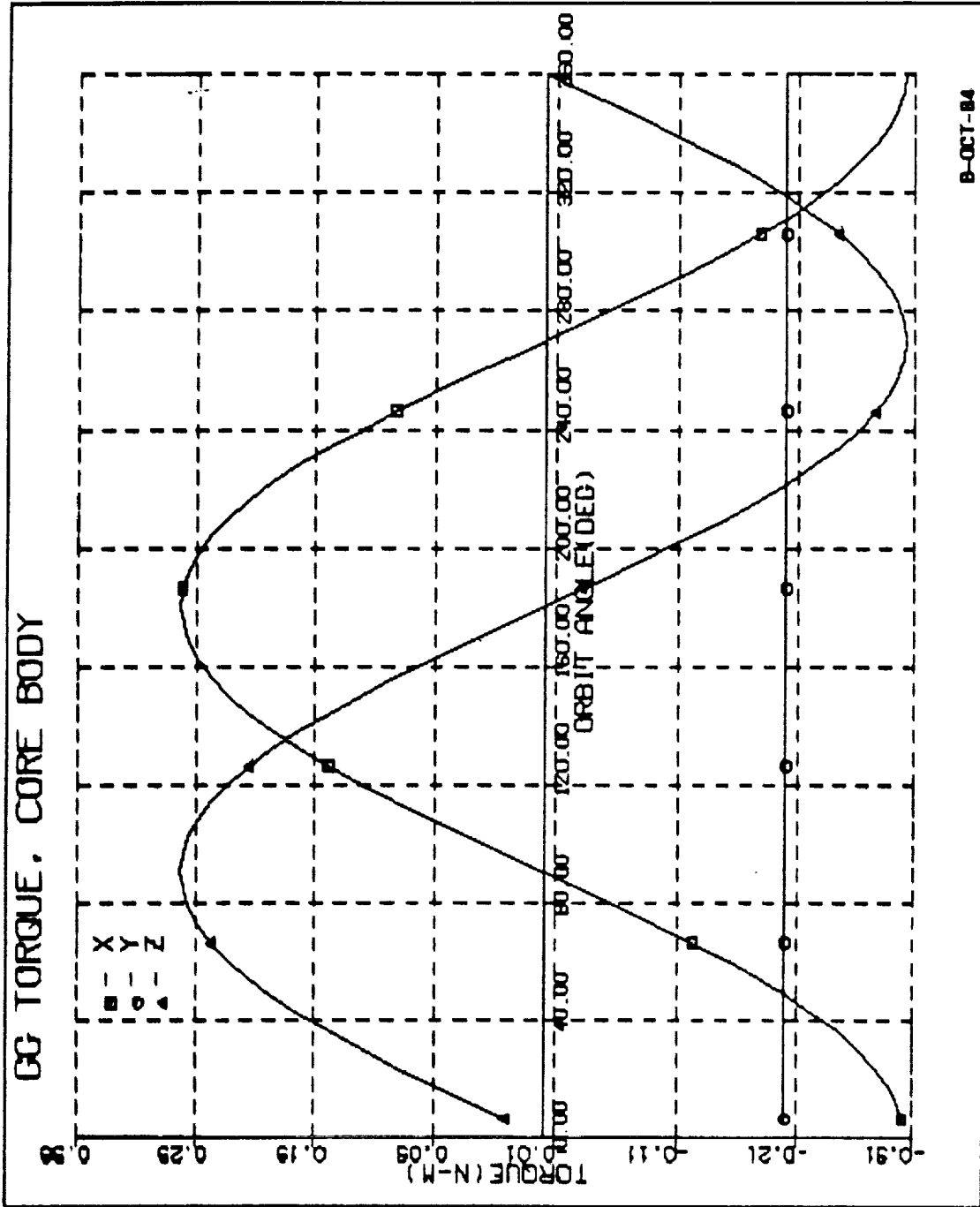


FIGURE 3 GG TORQUE, CORE BODY

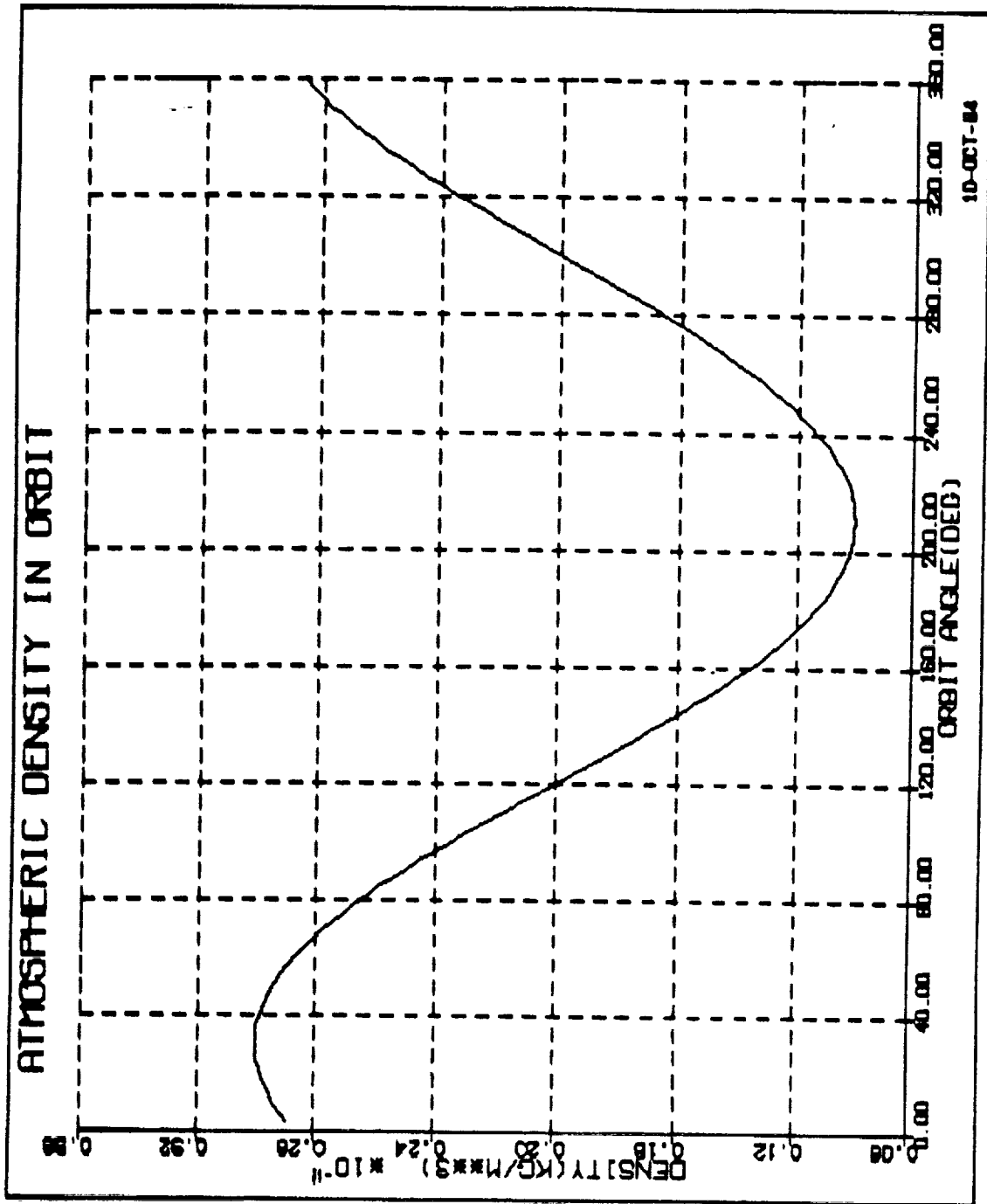


FIGURE 4 ATMOSPHERIC DENSITY IN ORBIT

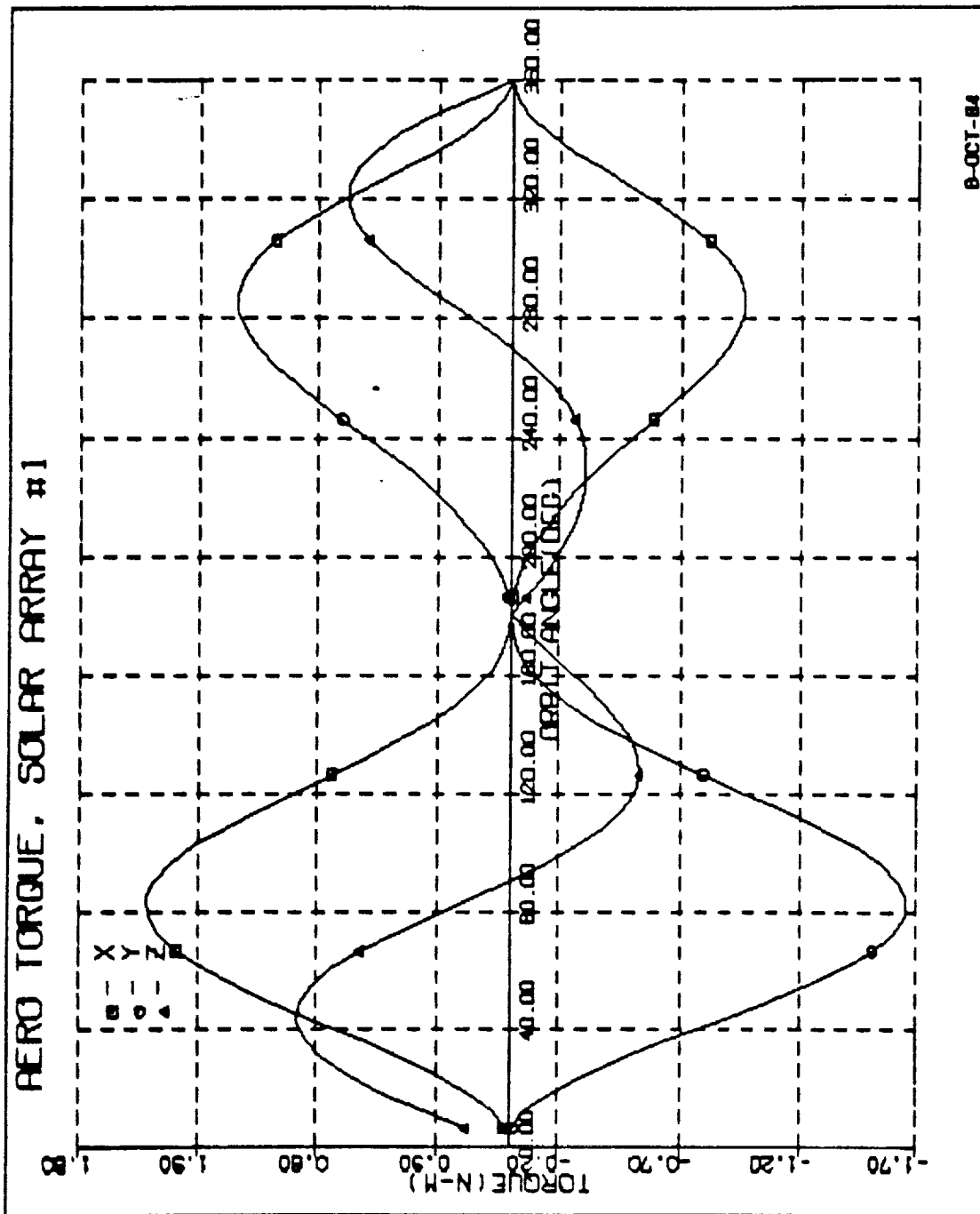


FIGURE 5 AERO TORQUE, SOLAR ARRAY #1

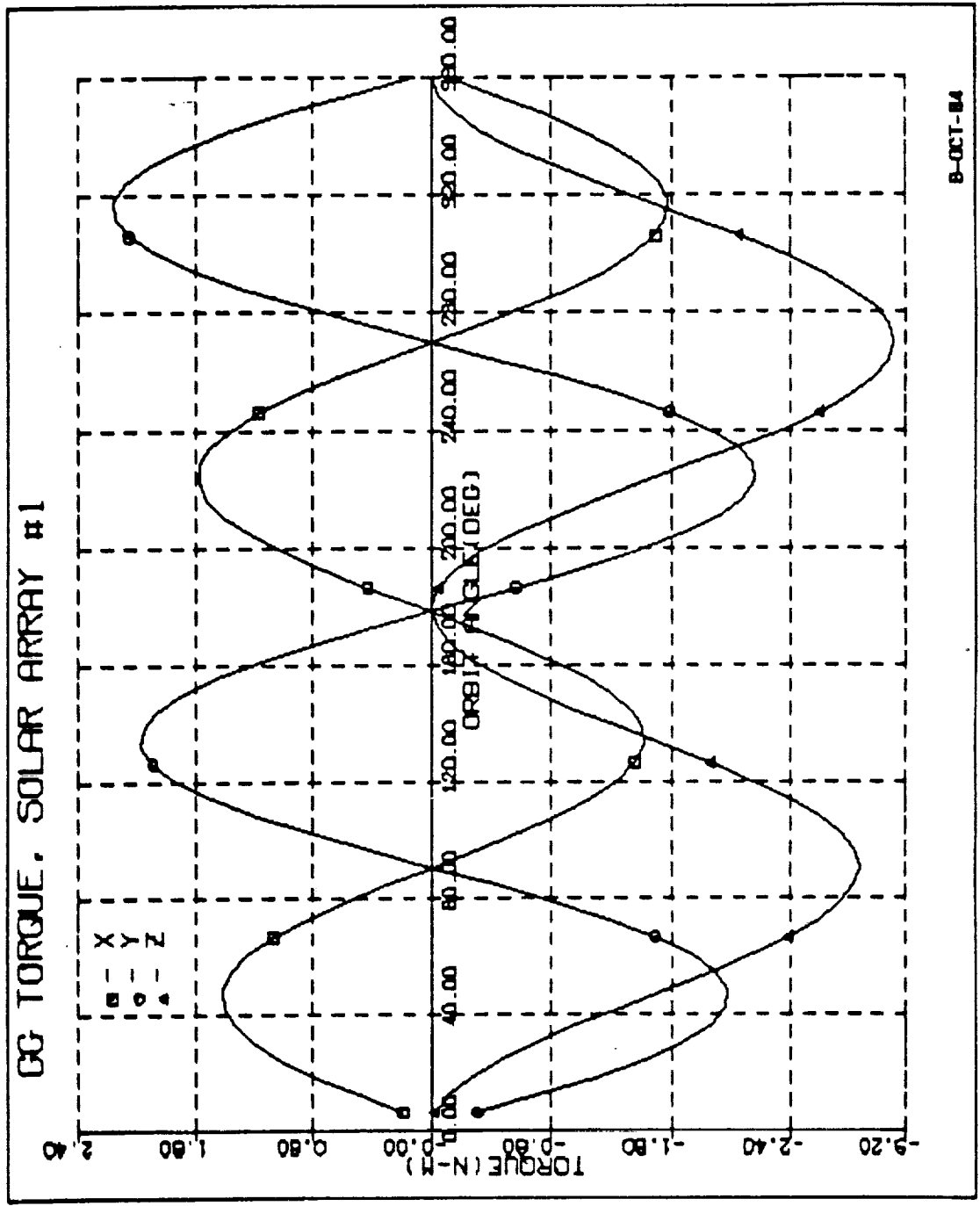
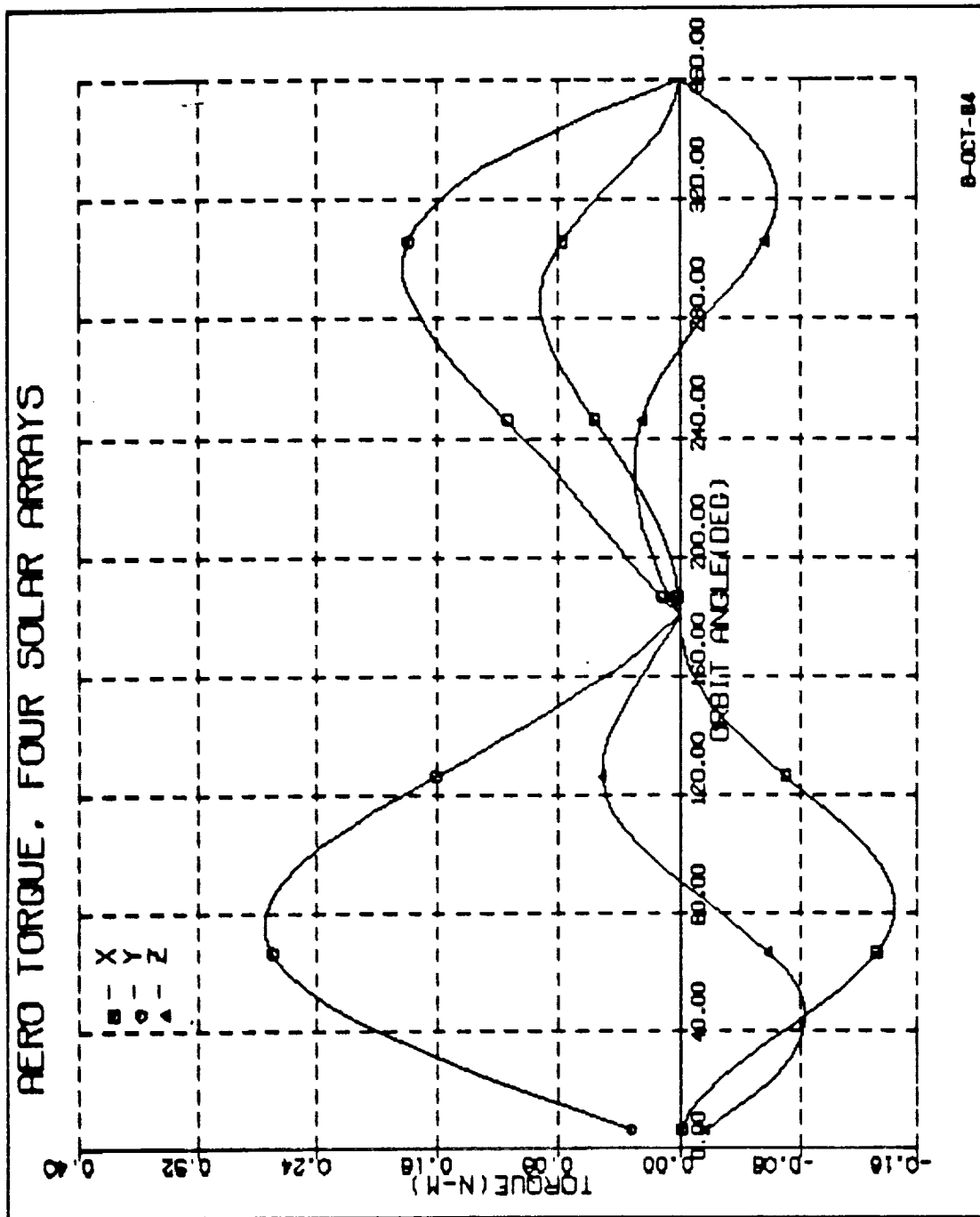
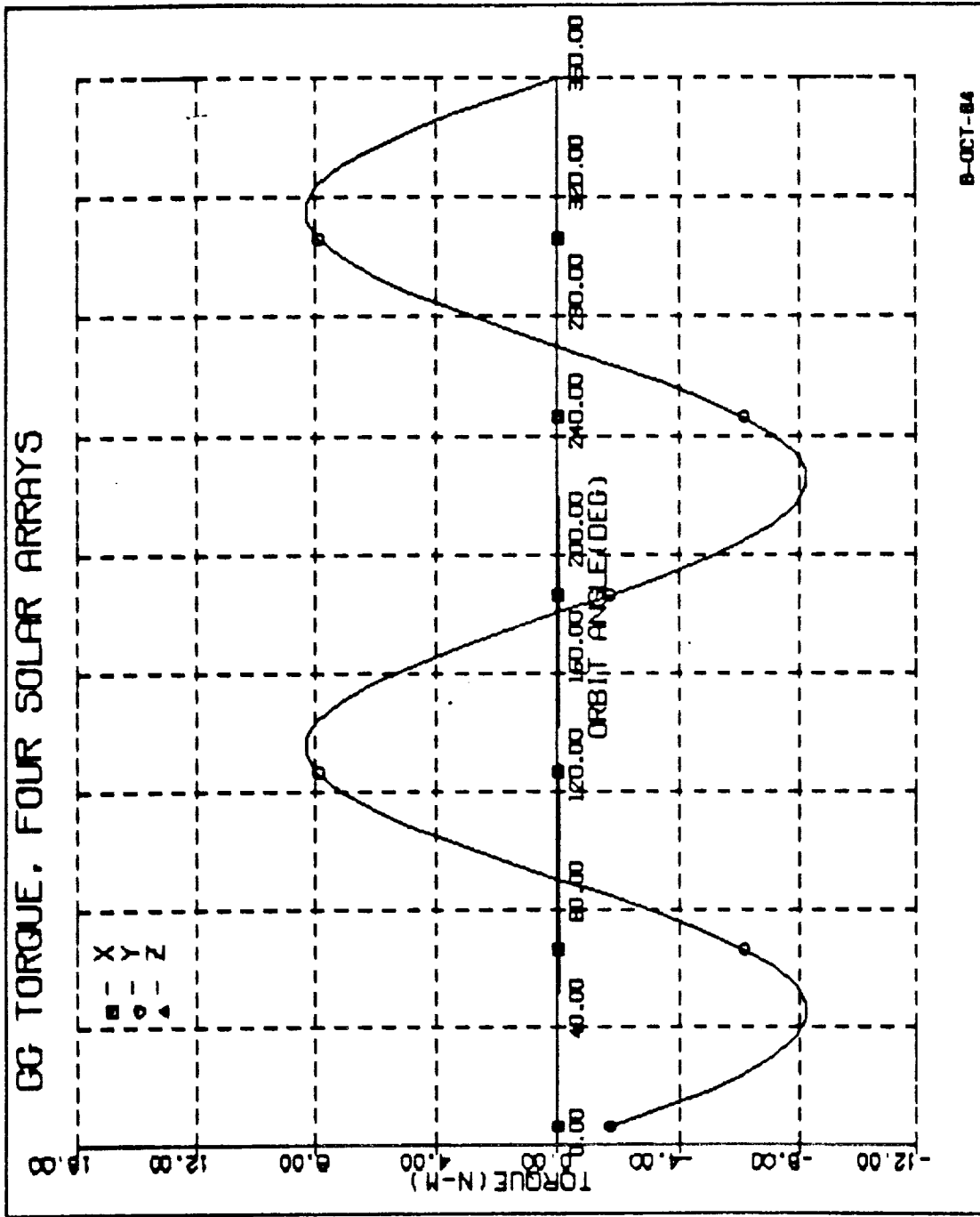


FIGURE 6 GG TORQUE, SOLAR ARRAY #1



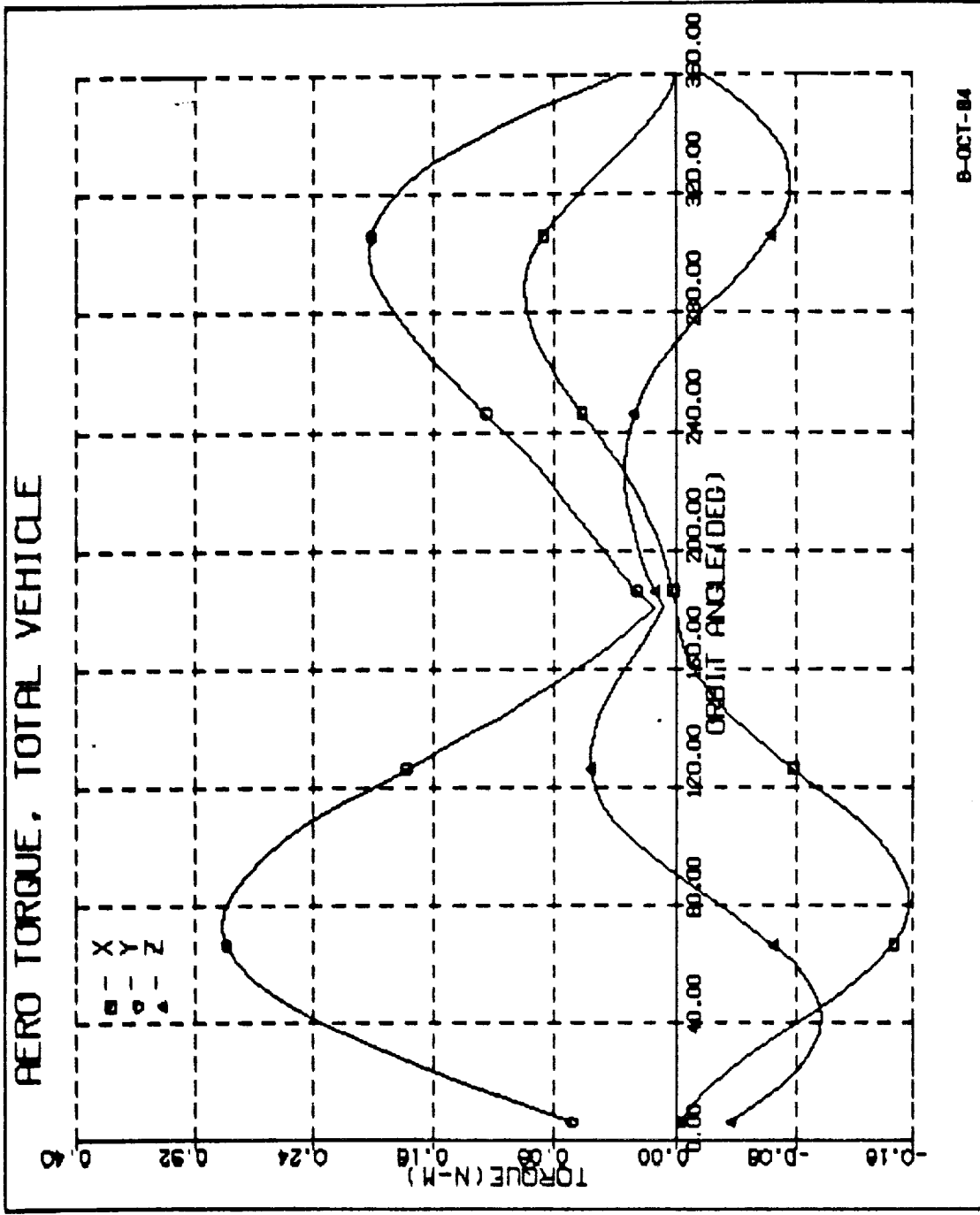
8-OCT-84

FIGURE 7 AERO TORQUE, FOUR SOLAR ARRAYS



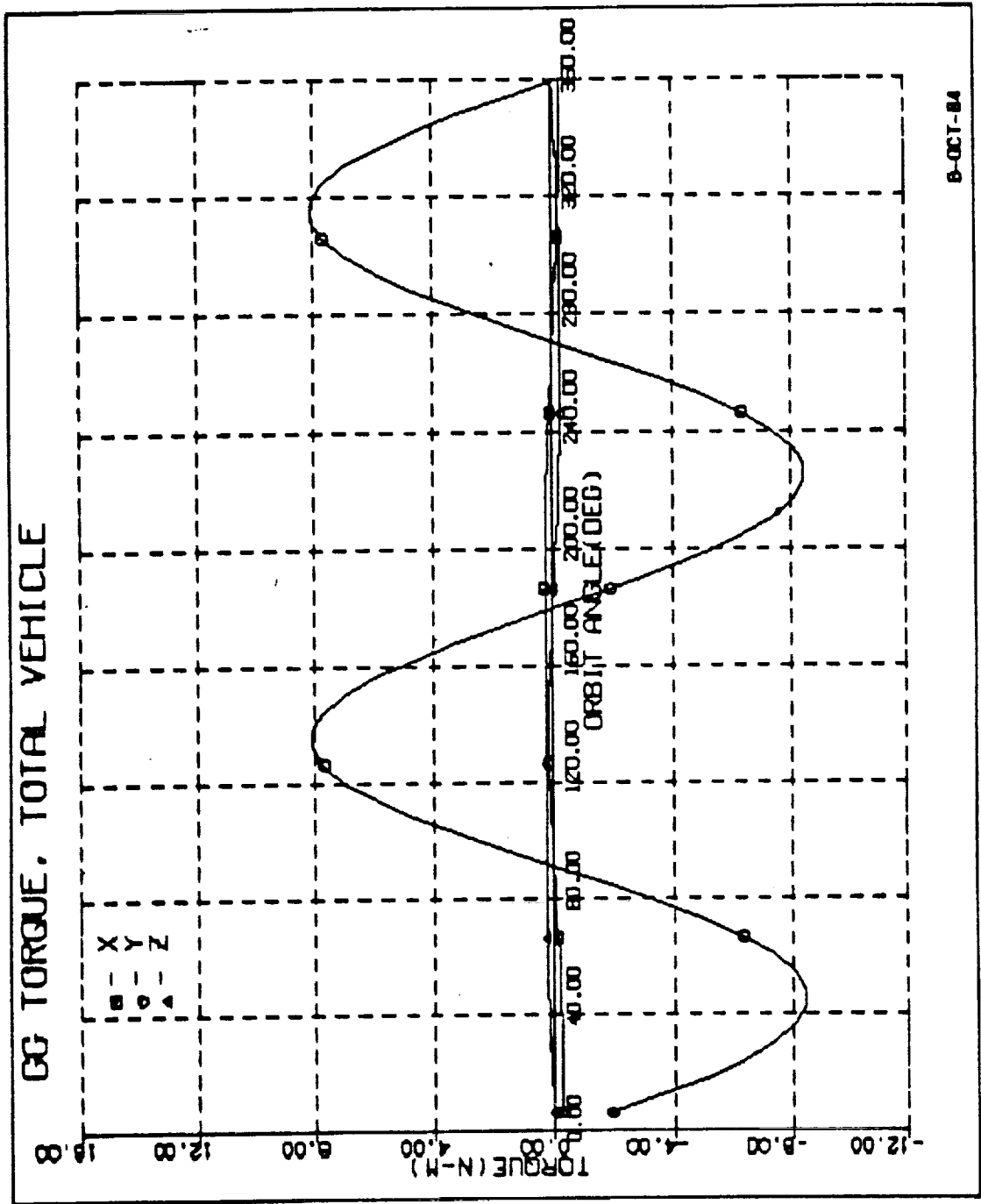
B-OCT-84

FIGURE 8 GG TORQUE, FOUR SOLAR ARRAYS



8-OCT-84

FIGURE 9 AERO TORQUE, TOTAL VEHICLE



B-OCT-84

FIGURE 10 GG TORQUE, TOTAL VEHICLE

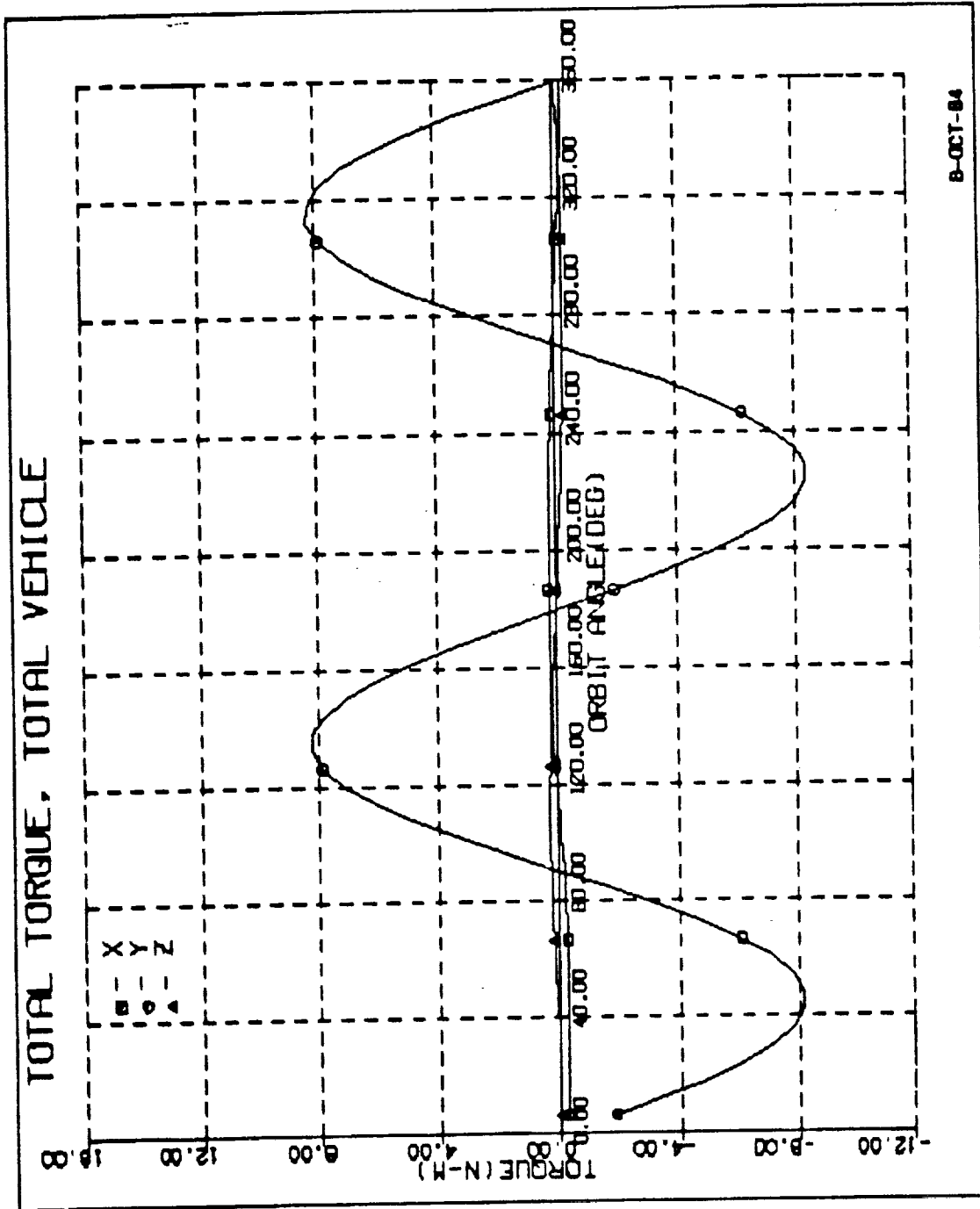


FIGURE 11 TOTAL TORQUE, TOTAL VEHICLE

due to the core body. The dominant IOP bias contribution is the solar arrays aero torque at a β -angle of zero while solar array GG torque dominates at β -angles of magnitude close to 45 degrees. Figure 12 shows the stored momentum profile if no momentum management were active and the initial momenta were -1000 N-m-s in Orbit Inertial (OI) X and Z respectively and -3600 N-m-s along the Y-axis which is perpendicular to the orbit plane (POP). The OI X-axis is along the velocity vector at noon and the OI Z-axis points up at noon. The start of all runs is orbital noon with the core body approximately trimmed to remove the POP bias torque.

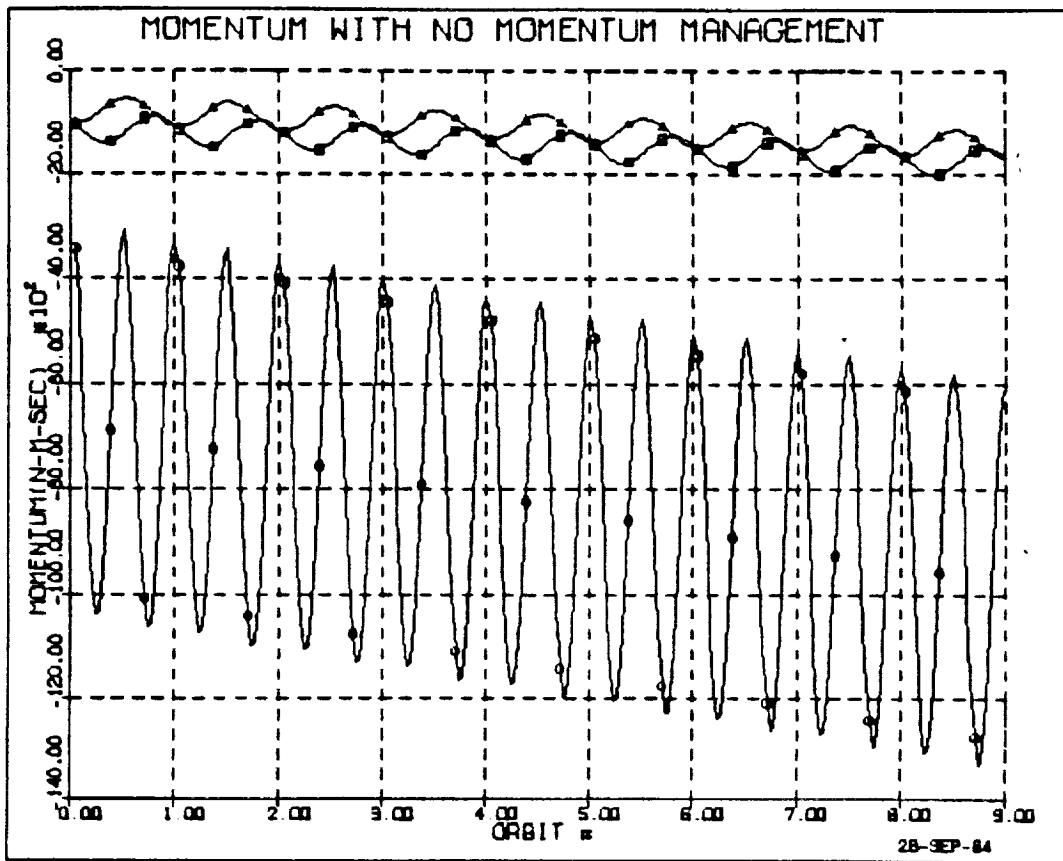


FIGURE 12 MOMENTUM WITH NO MOMENTUM MANAGEMENT

3.0 Techniques Considered

A known technique for bias counteraction is the use of magnetic torquing using four Space Telescope magnetic torquer bars. These would have the capability of generating approximately .13 N-m torque per axis when averaged over an orbit and are independent of vehicle configuration, attitude and atmospheric density. As their capabilities and control laws are known, including the disadvantages of weight, power and magnetic contamination, their use was not specifically investigated in this study but they remained the benchmark for innovative techniques. Several innovative techniques were investigated with various degrees of success. The emphasis of the study was to investigate in depth those techniques that appear promising. Among techniques that were investigated but eliminated were using the unwind profile of the radiator which did not generate sufficient torque. Modifying the pointing of various solar arrays using both the β -angle gimbal and the local vertical gimbal did not produce adequate desaturation without very large rotations during the dark side of the orbit which was considered undesirable from pointing performance. Off-nominal pointing of some of the solar arrays during daylight would produce undesirable power profiles.

The promising techniques developed to be described are use of the core body and the deployment of special aerodynamic appendages. All the techniques developed would be autonomous in the flight computer and simple to implement requiring only knowledge of inertias and approximate average atmospheric densities. Since the core body is maintained nominally local vertical (LV), its use for POP desaturation by means of gravity gradient torques is well known. The control laws for this will be described. Phased motions of the core body about the vehicle X-axis can be used to desaturate momentum IOP and will also be described. Initially, the control concept was to make these desaturation maneuvers every orbit. Results showed that after the initial transient decayed, the maneuvers were very small although payload pointing interference was still possible. Therefore an alternate control concept was to allow absolute momentum to approach a value inside its capability sphere. Only at this point would desaturation maneuvers of the core body be required although they would be much larger than those

performed each orbit. It appears that single orbit maneuvers performed every tenth orbit might be adequate after initial equilibrium is attained.

Using the appendages of Figure 13, no core body motion is required. Closed loop autonomous control laws for the angle of attack of these appendages have been developed. The appendages along the vehicle Y-axis desaturate the IOP momentum while the appendages along the Z-axis control the POP momentum. The hardware required to deploy and control these appendages could be adapted from solar array and antenna drives and does not represent new technology. The attainment of a given torque at a certain atmospheric density depends on the product of area times moment arm which could be traded off depending on considerations of weight, complexity and possible interference with payload pointing. The results of using these appendages compares favorably with magnetic desaturation in terms of weight, power, and complexity of both hardware and control laws. When atmospheric density is high, the baseline sized appendages produce greater desaturation capability than four Space Telescope torquer bars. During period of minimum density, the torquer bars have more capability but the requirements are less.

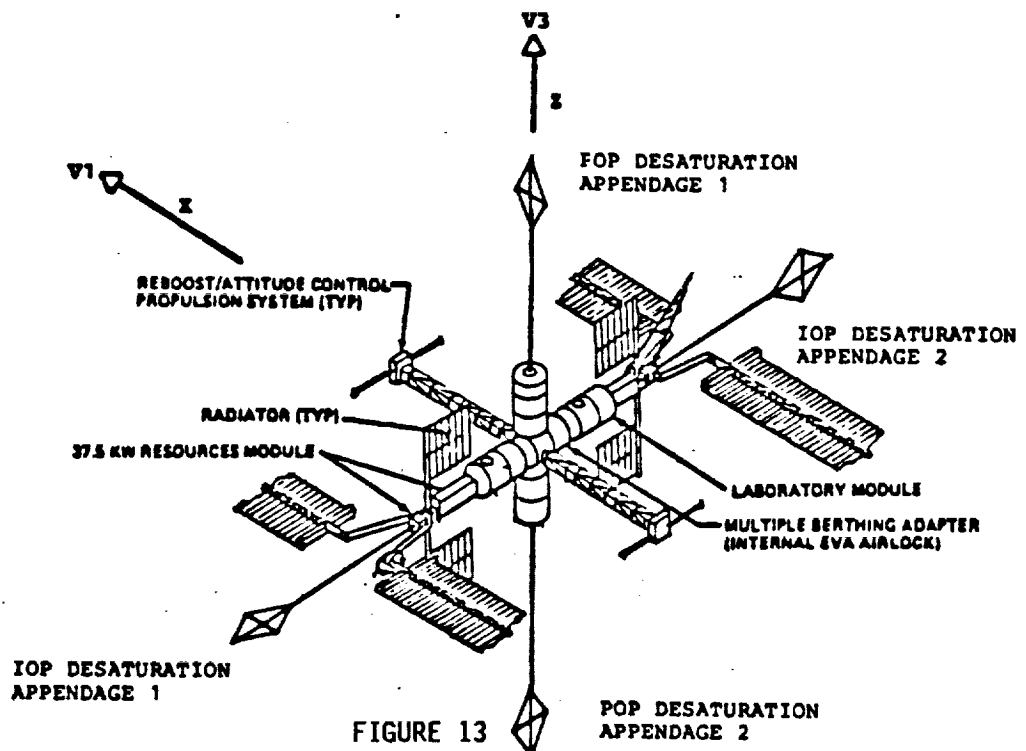


FIGURE 13
CDG PLANAR SPACE STATION WITH AERODYNAMIC DESATURATION APPENDAGES

4.0 Gravity Gradient Desaturation Using the Core Body

Utilizing the core body, which maintains an attitude relatively close to local vertical (LV) to desaturate the momentum perpendicular to the orbit plane (POP), is a technique previously investigated (ref 1). Assuming one principal axis is approximately POP and a second is approximately LV, the gravity gradient torque along the POP axis is given by equation 5. The total desired attitude change is the sum of that required to remove the bias and that required to center the momentum along the POP axis. The attitude change to counteract the bias torque is given by equation 6 which also utilizes the inverse of equation 5. The angle change required to center the momentum is given by equation 7. The new attitude about the POP axis is given by equation 8 and includes an effect for increased momentum due to the bias acting over an additional half orbit. This angle change is accumulated in the flight computer and while the core body attitude about the POP axis is controlled within a small range by the requirements of momentum management, the flight computer will, at all times, have knowledge of the actual attitude. Figure 14 shows a typical attitude about the POP axis while Figure 15 shows the momentum. The large initial changes about the POP axis occur due to the requirements of the centering logic.

$$T_{GGY} = 3\omega_0^2 \Delta I_2 \phi_p \quad (5)$$

$$\Delta\phi_1 = \frac{(1-z^{-1})H_y}{3\omega_0^2 T_0 \Delta I_2} \quad (6)$$

$$\Delta\phi_2 = \frac{H_y}{3\omega_0^2 T_0 \cdot \Delta I_2} \quad (7)$$

$$\phi = z^{-1}\phi_y - 1.5\Delta\phi_1 - \Delta\phi_2 \quad (8)$$

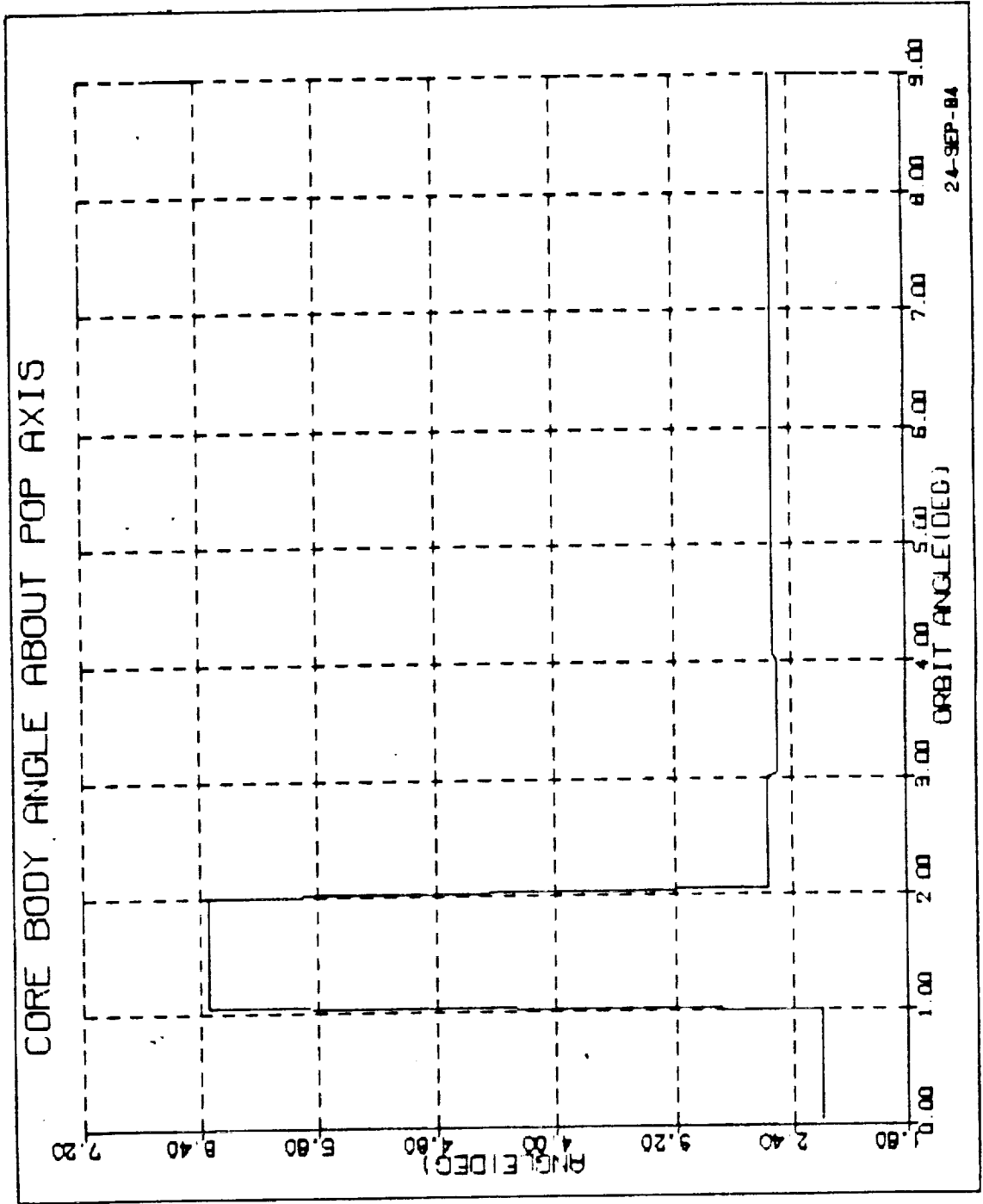
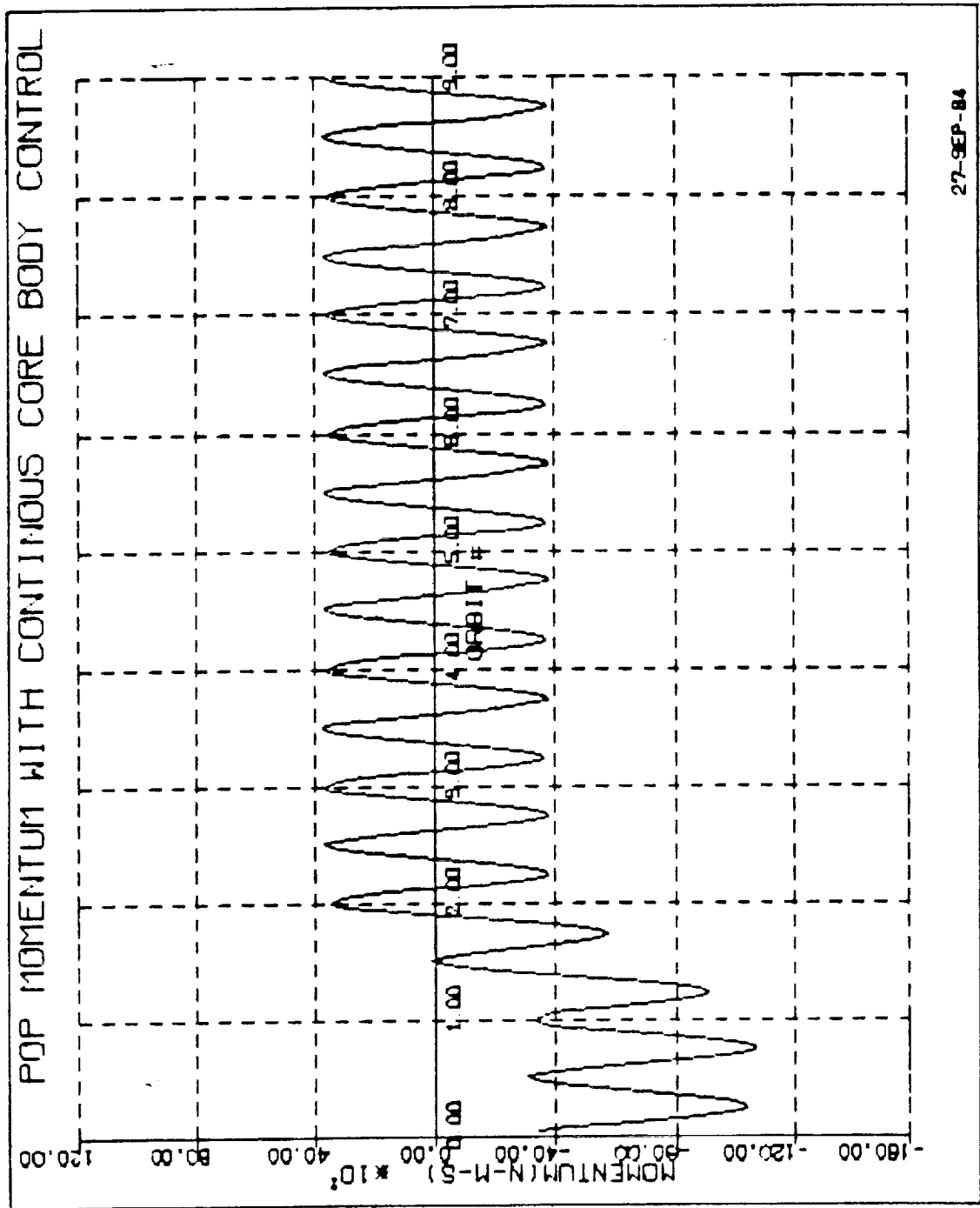


FIGURE 14 CORE BODY ANGLE ABOUT POP AXIS



27-SEP-84

FIGURE 15 POP MOMENTUM WITH CONTINUOUS CORE BODY CONTROL

If the vehicle Z-principal axis is moved out of the orbit plane by a rotation about the vehicle X-axis, a body fixed gravity gradient torque about the X-axis will be produced. However this torque is cyclic about two axes fixed in the orbit plane. In order to generate a gravity gradient bias torque in the orbit plane, it is necessary to generate a phased rotation about the vehicle X-axis. If the orbit inertial (OI) axes have average momenta over the previous orbit given respectively by H_x and H_z the total bias torque to be generated about the OI X and Z axes are given by equations 9 and 10. The magnitude of the total IOP torque is given by equation 11 and the direction of the desired torque is given by equation 12.

$$T_{Dx} = \frac{-\bar{H}_x}{T_o} \quad (9)$$

$$T_{Dz} = \frac{-\bar{H}_z}{T_o} \quad (10)$$

$$T_{DIOP} = \sqrt{T_{Dx}^2 + T_{Dz}^2} \quad (11)$$

$$U_T = \tan^{-1} \left(\frac{T_{Dx}}{T_{Dz}} \right) + \frac{\pi}{2} \quad (12)$$

After the desired magnitude and direction of the IOP torque to be generated is calculated, the second part of the calculation is the definition of the vehicle attitude profile with respect to the orbital plane. Instantaneously, the gravity gradient torque in body space is given by equation 5 with ΔI_1 replacing ΔI_2 . If that attitude is maintained over one-half orbit centered about a given direction, the average torque in that direction is given by equation 13 while the average torque in the perpendicular direction (equation 14) is zero. Reversing the rotation about the X axis during the other half of the orbit produces a rectified torque in the desired direc-

tion and still zero in the orthogonal direction. The angle required to desaturate the IOP bias is given by equation 15 which shows an efficiency loss of $2/\pi$ compared with the angle required for POP gravity gradient desaturation. Examining Figure 16, which shows the IOP momentum with core body desaturation active, indicates that the average values of OI X and Z momenta impose only small momentum storage requirements on the CMGs and that the bias torques are removed. Figure 17 shows a typical core body rotation profile about its X-axis for IOP desaturation which shows that after the transients have decayed, the required angles are quite small and that even maneuvering at .01 deg/sec, the times to attain the new attitudes are negligible.

$$\tau_D = \frac{3\omega_0^2 \theta \Delta I_1}{\pi} \int_{U_T - \frac{\pi}{2}}^{U_T + \frac{\pi}{2}} \cos(U - U_T) dU = \frac{3\omega_0^2 2\theta \Delta I_1}{\pi} \quad (13)$$

$$\tau_L = \frac{3\omega_0^2 \theta \Delta I_1}{\pi} \int_{U_T - \frac{\pi}{2}}^{U_T + \frac{\pi}{2}} \sin(U - U_T) dU = 0 \quad (14)$$

$$\theta = \sin^{-1} \left(\frac{\pi \tau_{OIOP}}{3\omega_0^2 2 \cdot \Delta I_1} \right) \quad (15)$$

It should be noted that since torque and momentum are not in the same direction, it is difficult to remove both bias and average values of the momentum in two OI axis. However the average momenta are at values close to zero and in maintaining those values with the control law, bias torques are also counteracted. Examining the POP rotations of Figure 14 and the IOP profile of Figure 17 shows that after the momentum along POP is centered and the bias is removed, both the POP corrections required and the IOP profiles represent small angles which, nevertheless, could disturb payload pointing. Due to the balanced structure of the vehicle, the momentum

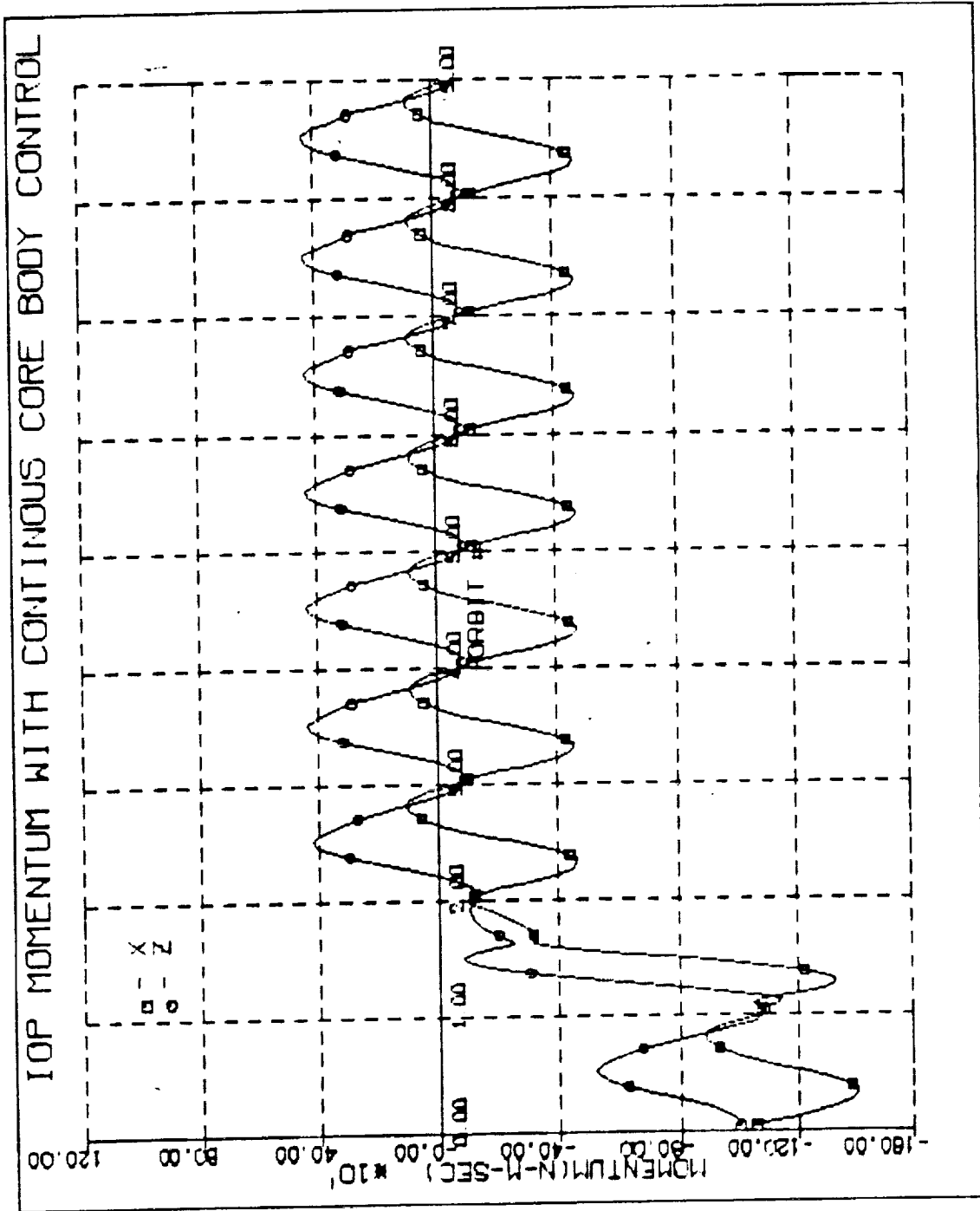
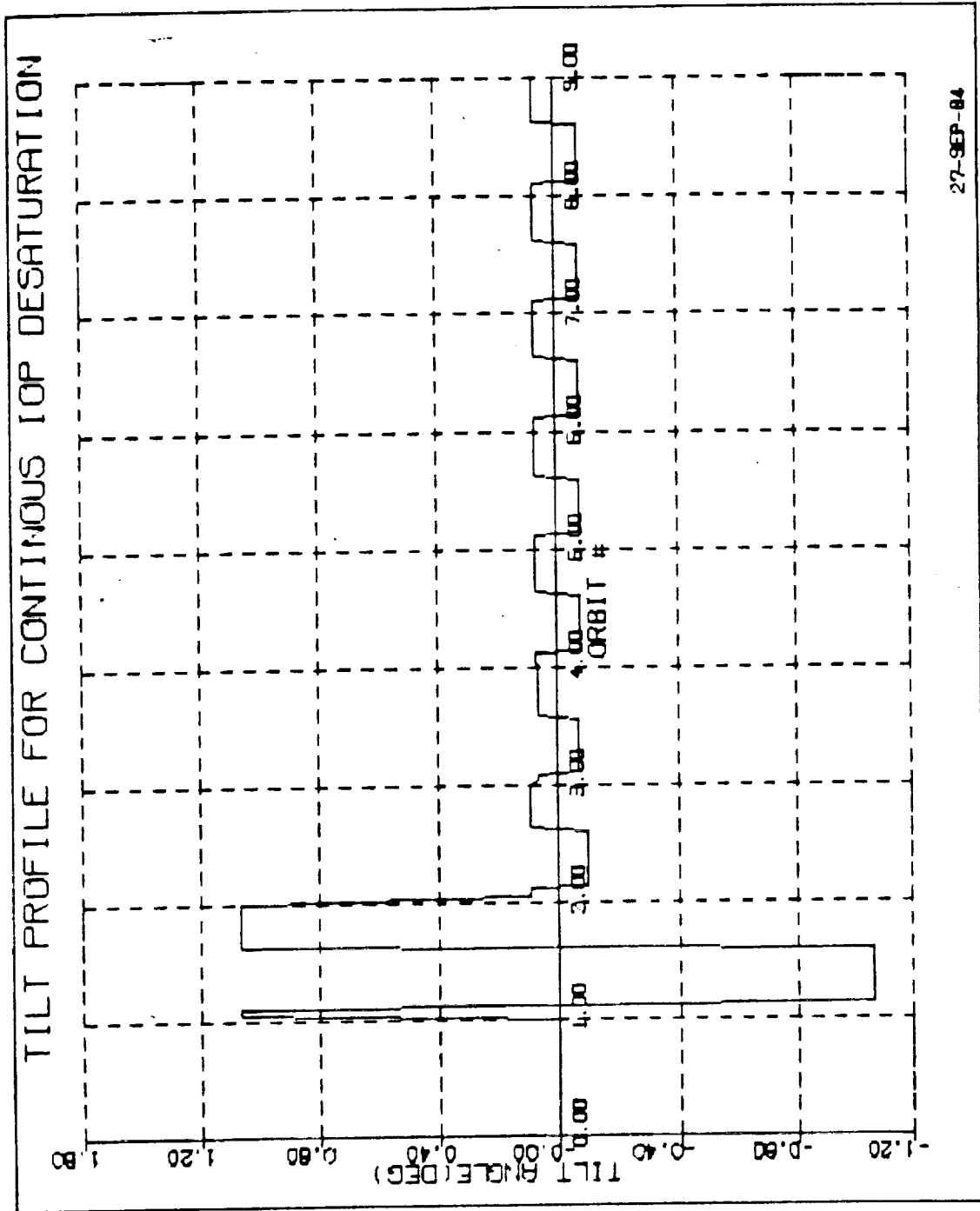


FIGURE 16 IOP MOMENTUM WITH CONTINUOUS CORE BODY CONTROL



27-SEP-84

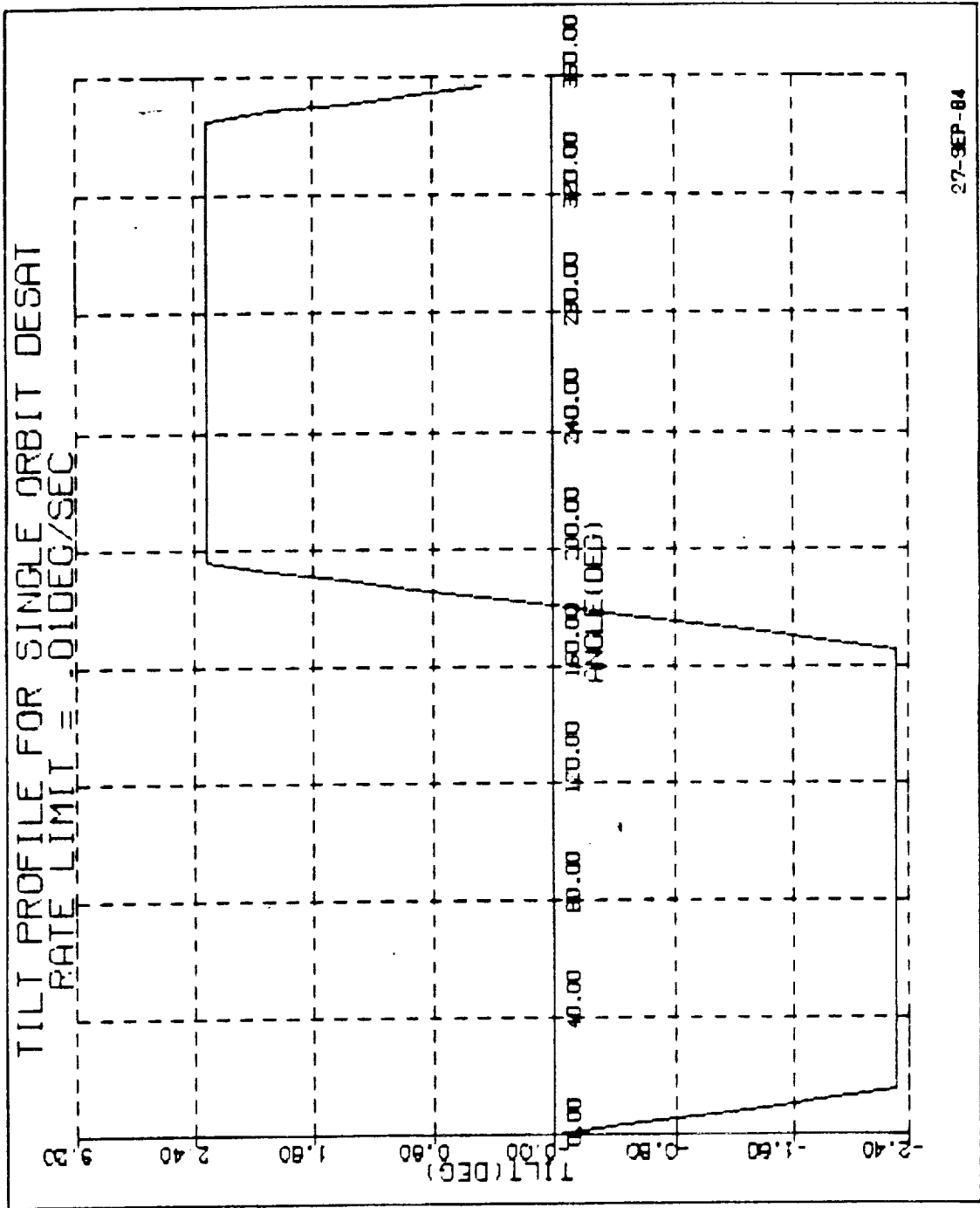
FIGURE 17 TILT PROFILE FOR CONTINUOUS IOP DESATURATION

accumulation, on a per orbit basis, is very low once POP bias has been removed by the appropriate rotation of the core body. This led to the development of an alternate method of gravity gradient desaturation using the core body. Instead of performing an adjustment every orbit, the vehicle was held inertially fixed until the absolute momentum attained a software limit. The maximum momentum storage capability of four Skylab type Control Moment Gyro (CMG) is 12000 newton-meter-seconds (N-m-s) leading to the selection of a software limit set at 9000 N-m-s. The logic was set so that if the stored absolute momentum attained this value, corrective action for both POP and IOP momentum would be performed.

The amount of momentum left for maneuvering is quite low so that a maximum core body maneuvering rate of .01 deg/sec about any vehicle axis was assumed. Since the angles required for desaturation will be much larger when momentum is allowed to go to the inside of the 9000 N-m-s momentum sphere, the assumption of square wave attitude angle profiles of Figure 16 for IOP desaturation can no longer be made. Therefore with the assumed maximum core angle with infinite rate capability calculated, the actual angle is adjusted for finite rate according to equation 16. This maintains the same integral of area x time as if the new attitude were attained instantaneously leading to the trapezoidal profile of Figure 18.

$$\theta' = \frac{\dot{\theta}_{\max}(T_o/2)}{4} \left(1 - \sqrt{1 - \frac{8\theta}{\dot{\theta}_{\max}(T_o/2)}} \right) \quad (16)$$

These considerations are less critical for the new angle about the POP axis. Desaturation about the POP axis is not dependent on angle in orbit for the adjustment of the momentum states. Therefore finite maneuvering times will compensate at the beginning and end of the desaturation profile. Due to the significant time required for the completion of the single orbit IOP desaturation, it was decided to perform a maneuver in only two steps as shown in Figure 18 rather than the three steps of Figure 17. It should be noted that Figure 18 shows the desaturation profile IOP from time of start, which could be any time in orbit, and assuming the calculations are performed at a fixed position in orbit, the end of the desaturation could take



27-SEP-84

FIGURE 18

TILT PROFILE FOR SINGLE ORBIT DESATURATION, RATE LIMIT = .01 DEG/SEC

two orbits from the time that the calculations are made. The other change in IOP desaturation when no longer performed at orbital frequency is, rather than drive the IOP momentum to zero when desaturation is required, the momentum will be driven to the opposite point on the IOP momentum circle given by equations 17 and 18. Since the bias should drive the momentum in the same direction as previously, the maximum time allowed before the next desaturation is required should be extended. Figure 19 shows the momentum IOP about two inertial axis with single orbit desaturation.

$$T_{Dx} = \frac{-2\bar{H}_x}{T_0} \quad (17)$$

$$T_{Dz} = \frac{-2\bar{H}_z}{T_0} \quad (18)$$

The single orbit POP desaturation technique utilizes only minor modifications to the POP desaturation technique at orbital frequency. The angle to remove the bias is given by equation 6 and that remains as the new vehicle attitude until the next desaturation is required. The angle to center the momentum is given by equation 7 and that angle is removed at the conclusion of the single orbit desaturation. The new angle at the beginning of a desaturation is given by equation 19 and that at the end of one desaturation period is given by equation 20. The period of the single orbit POP desaturation is concurrent with that of IOP desaturation which generally is not the position (orbit noon) where the calculations are performed.

$$\phi = z^{-1}\phi - 1.5\Delta\phi_1 - \Delta\phi_2 \quad (19)$$

$$\phi = z^{-1}\phi + \Delta\phi_2 + .5\Delta\phi_1 \quad (20)$$

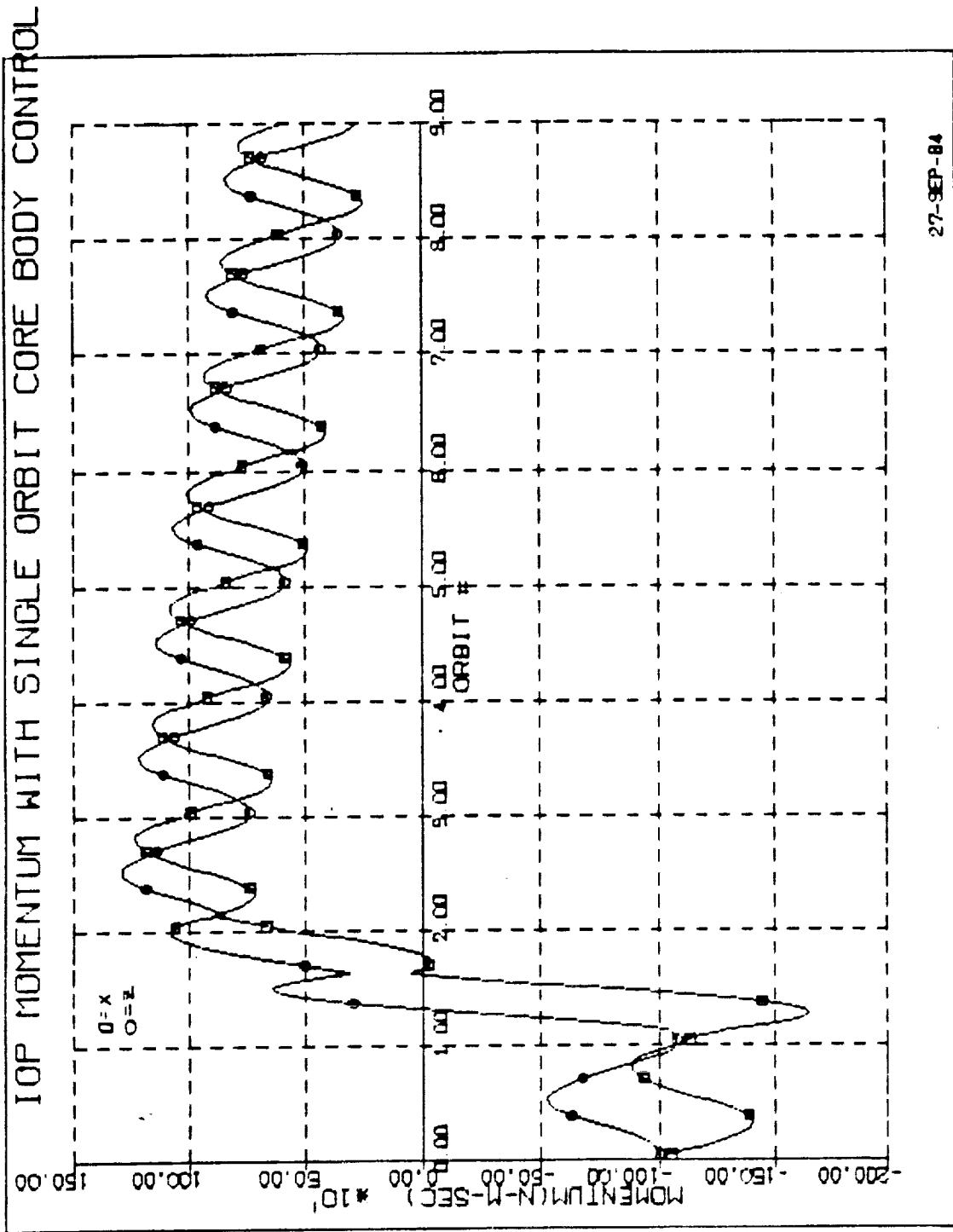
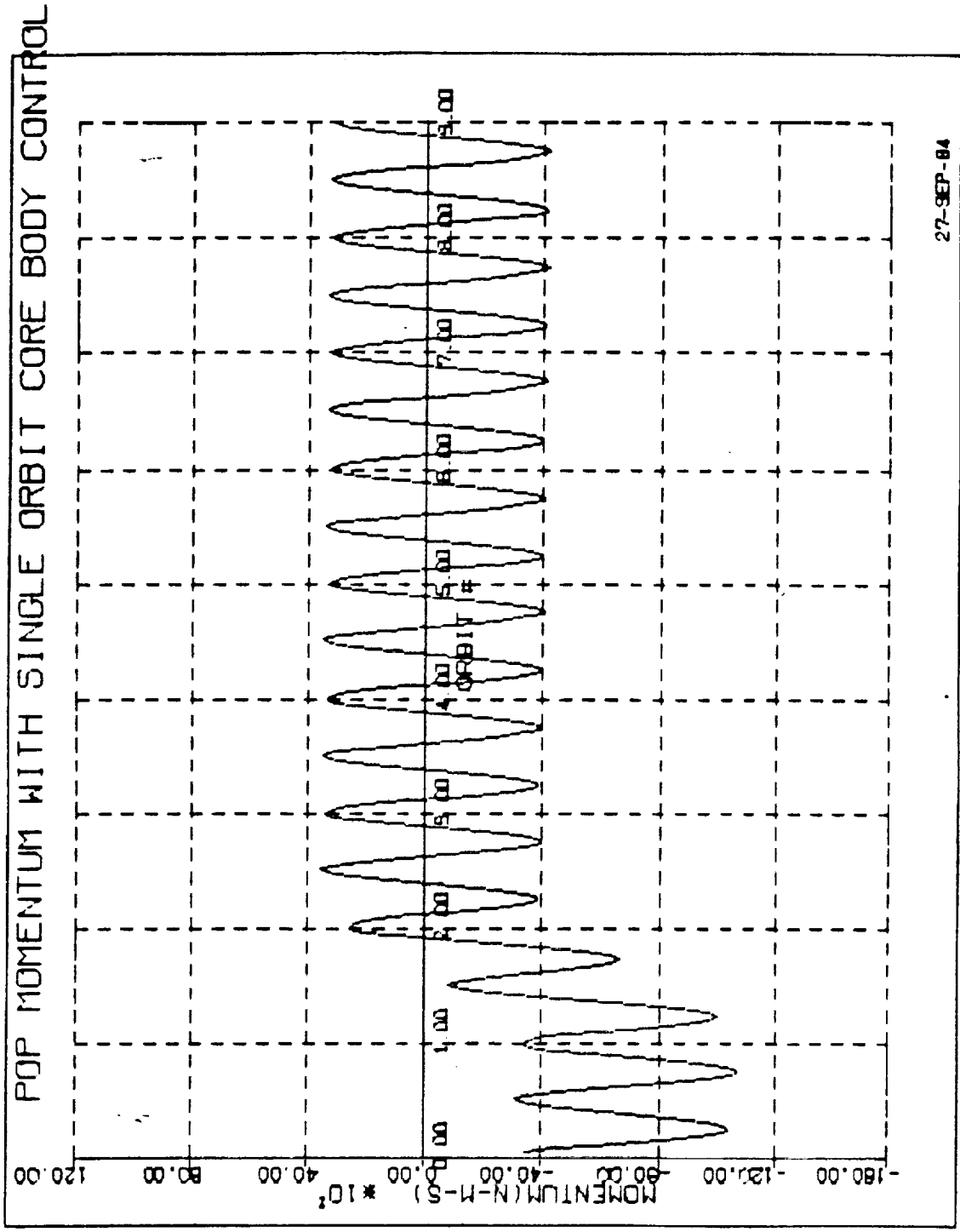


FIGURE 19 IOP MOMENTUM WITH SINGLE ORBIT CORE BODY CONTROL

The POP attitude maneuver at the beginning of the single orbit desaturation is the sum of the bias removal and momentum centering angles while that at the conclusion is the negative of centering angle. Using the momentum desaturation technique of allowing absolute momentum to reach the maximum allowable value of 9000 N-m-s, the POP momentum with single orbit desaturation is shown in Figure 20. A subsequent desaturation was not required for 30 orbits which is probably too optimistic for a real mission as simulation did not include varying β -angle, atmosphere density and mass properties between successive orbits. The real trimming of torque and momentum will probably not be as accurate as shown in the simulation. However even the attainment of ten orbits of pure Inertial Hold before momentum management trim maneuvers might represent adequate viewing time for many payloads.

Another desaturation technique, magnetic desaturation using the control laws developed during the Space Platform study was considered but not actually investigated in detail for Space Station. These control laws would be directly applicable to Space Station and the magnitudes of the IOP bias torques (.05 N-m) on OI X and Z are well within the capability of four Space Telescope torquer bars. However the .5 N-m bias torque about the POP axis is beyond the capability of 4 bars unless the vehicle is first trimmed by a closed loop POP axis rotation. Magnetic desaturation also has undesirable properties such as the weight and power required and the potential for magnetic contamination of payloads.

Two alternate desaturation techniques would be mass shifting for gravity gradient desaturation and appendage control for aerodynamic desaturation with the latter considered more promising. The appendages considered for this study are two flat plates along \pm vehicle Y-axis for IOP desaturation and two flat plates along \pm vehicle Z-axis for POP momentum trimming. It was decided that the magnitude of the POP bias was too large for complete aerodynamic desaturation and the flat plates would act as trim tabs after several orbits of gravity gradient maneuver desaturation about the POP axis. This report will discuss sizing, control laws and show closed loop results of aerodynamic desaturation using flat plate appendages. In addition, results will be shown for those cases where the atmosphere is different from the nominal density used to size the appendages and control law gains.



27-SEP-84

FIGURE 20 POP MOMENTUM WITH SINGLE ORBIT CORE BODY CONTROL

5.0 Aerodynamic Desaturation Using Flat Plate Appendages

Simulation results have indicated that for the baseline vehicle inertias, baseline offsets of the center of mass from the center of symmetry and the baseline atmosphere model ($\rho_{avg} = 1.73 \times 10^{-12} \text{ kg/m}^3$, $K_{db} = .5$, $U_{db} = 30$ degrees), the OI X and Z bias torques are about .0135 N-m each and the magnitude of the total IOP bias torque which is the vector sum of the components is about .02 N-m at a zero degree β -angle. However at a non-zero β -angle, although the aerodynamic forces and torques are less, the gravity gradient bias IOP is greater. The worst case IOP bias torque occurred at a β -angle of -45 degrees about the X-axis. This can be realized intuitively that as the solar arrays are rotated from POP for the β -angle, a gravity gradient bias torque along the OI X-axis is generated having its maximum value at 45 degree magnitude β -angle. For the inertias and cm used, the magnitudes of the aerodynamic and gravity gradient biases add about the OI X-axis at the negative β -angle producing the worst case torque of .045 N-m consisting of 0.035 N-m gravity gradient and 0.01 N-m aerodynamic torque. Using the efficiency factor of $2/\pi$ (to be shown later) which is identical to that for IOP desaturation using the core body, the required torque from the panels would be about .075 N-m. To allow margin, the panels for IOP desaturation were sized to generate T_{nom} of 0.1 N-m. Assuming an orbital velocity squared of $5.8 \times 10^7 \text{ meters}^2/\text{sec}^2$ and a drag coefficient (C_d) of two, the product of area times moment arm must equal 1000 meters cubed to generate T_{nom} . Typically, this would represent an area of 40 square meters with a 25 meter moment arm or 20 square meters with a 50 meter moment arm.

The sizing requirements for the POP axis trim tabs is less clear-cut as requirements depend on the degree of trim attained by gravity gradient desaturation using the core body. In order to simplify hardware considerations, it was decided to use the same requirements as for IOP desaturation, namely T_{nom} torque capability at an atmospheric density of ρ_{nom} . In the POP axis

aerodynamic torque, the unfavorable factor of $2/\pi$ for the theoretical torque achieved in the desired direction does not exist so the torque attained could be T_{nom} . Referring to Figure 13, panel 2 generates a positive torque about the POP axis. The general requirements for deployment and rotation of the panels are consistent with solar array and antenna mechanisms. Candidates for actuators include stepping motors and torquers. Since the vehicle is rotating at orbital rate, in order to maintain a fixed orientation to the air flow, the panels must only be rotated when reorientation is required. This could favor stepper motors as actuators since the devices would be off when not actually rotating. An estimate of the weight is 15kg for each actuator/boom/panel or 60 kg for the system.

The control law for IOP desaturation was based on assuming a constant atmospheric density and sampling the momentum of the two IOP axis at orbital frequency with the sampling performed at orbital noon. The choice of noon for momentum sampling is arbitrary for this simulation only. Perhaps midnight which was used in Skylab for Ephemeris updating would be operationally preferable but results should be independent of sampler placement in orbit. The requirement of knowledge of average density makes the aerodynamic desaturation somewhat less desirable than gravity gradient desaturation. Currently, the inertia matrix of a spacecraft is assumed to be well known while atmospheric data at the Space Station altitude is known best from its long term averages. Therefore the study involving aerodynamic desaturation with flat appendages will consider the case where the control law estimate of ρ_{avg} is different from the "real" atmospheric density. It will be shown that momentum desaturation is still viable even with a certain amount of mismatch. The density variations within the orbit, due to the diurnal bulge are less critical than the average value of the density for aerodynamic desaturation and because of the uncertainty of the exact density distribution during an orbit, are not included in the control law.

The momentum sampling scheme for the generation of the required torques follows along the same general lines as those used for the core body desaturation with the IOP bias torques to be counteracted given by equations 9 and 10, the magnitude of the total bias torque to be generated is given by equation 11 while the direction of the desired torque is given by equation 12.

Figure 21 shows the two appendages for IOP desaturation with 2 "on" and 1 feathered producing a negative torque about the vehicle Z-axis. When appendage 1, along vehicle +Y-axis is rotated perpendicular to the air flow, a positive torque about vehicle Z is generated. The appendages which develop torque along the vehicle Z-axis IOP are along the two ends of the vehicle Y-axis with their axis POP. The control law developed for IOP desaturation admits only three states for the two appendages: both feathered, appendage 1 perpendicular and 2 feathered and 1 feathered and 2 perpendicular to the velocity vector. Therefore only three torque states about Z-vehicle axis are possible. These are zero torque if both or none of the appendages were feathered, and maximum magnitude if only one appendage is feathered. The zero torque condition will be assumed by both appendages feathered. If the same appendage were perpendicular to the air flow for the entire orbit, the torque would be a bias in vehicle space but cyclic in IOP axes. Therefore it will be necessary to develop a control law involving feathering each panel part of the orbit and possibly both panels part of the orbit to generate a torque with desired magnitude and direction.

It is assumed in this study that the separation of the cm from the cp is negligible compared to the moment arm of the individual appendage and given identical densities, the torques due to each appendage would have the same magnitude. It was also assumed for this study that the appendages do not affect the gravity gradient torques. A typical case that is also easy to visualize is a β -angle of zero where the bias torques are $-.014$ N-m about both OI X and Z axes. This also represents a torque of magnitude $.02$ N-m about an axis 315 degrees from noon. In order to counteract this external bias, the appendages should generate a positive torque along an axis 45 degrees from noon without any component along a perpendicular axis.

This is done by using panel 1 symmetrically about 315 degrees and panel 2 about 45 degrees. All subsequent calculations are based only on density equal to ρ_{nom} with closed loop calculations taking care of actual atmospheric density. The theoretical torques generated are symmetrical in 4 quadrants about the torque direction so the equation for turning panels on is given only for two quadrants symmetric about the desired torque direction.

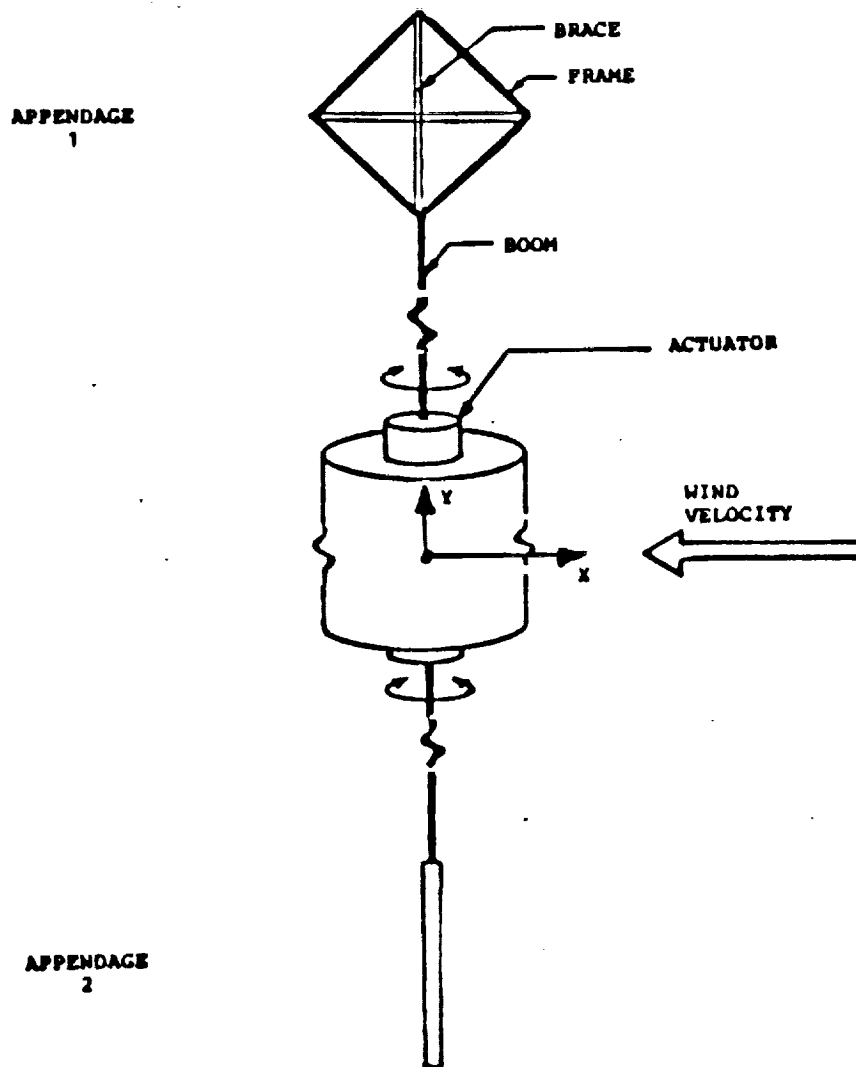


FIGURE 21 IOP DESATURATION APPENDAGES

The average torque in the desired direction over one half orbit is given by equation 21. If a certain magnitude is desired, the inverse of equation 21 is solved for the angle U_{on} which represents the "on time" of the appendage torque IOP. This angle is given by equation 22. The maximum torque that can be generated in the desired direction if the angle is ninety degrees is $T_{nom} \times 2/\pi$. The torque in the direction perpendicular to the desired torque is given by equation 23 and can be seen to be zero if ρ is actually constant.

$$T_D = \frac{T_{nom}}{\pi} \left(\frac{\rho_{est}}{\rho_{nom}} \right) \int_{U_T - U_{on}}^{U_T + U_{on}} \cos(U - U_T) dU = \frac{2T_{nom}\rho_{est}}{\pi\rho_{nom}} \sin(U_{on}) \quad (21)$$

$$U_{on} = \sin^{-1} \left(\frac{\pi \cdot \rho_{nom} T_{DIOP}}{2 \cdot \rho_{est} T_{nom}} \right) \quad (22)$$

$$T_{\perp} = \frac{T_{nom}}{\pi} \left(\frac{\rho_{est}}{\rho_{nom}} \right) \int_{U_T - U_{on}}^{U_T + U_{on}} \sin(U - U_T) dU = 0 \quad (23)$$

The POP axis control contains an integral path so the desired setting is the sum of a bias and integral path. The bias contribution to the desired POP torque is given by equation 24 while the desired centering torque is given by equation 25. The total torque desired is the sum of the bias and centering torques. The POP axis trim tabs control law utilizes a different approach from the IOP control law. Either panel 1 or panel 2 is "on" the entire orbit with the same angle based on the POP momentum sample. Unlike the IOP control law, the panel that is "on" can be set at any angle between zero and ninety degrees. The magnitude of the torque is determined by equation 26 while the angle that the normal to the panel makes with the airflow to generate the desired torque is given by equation 27.

$$T_{By} = -\left(\frac{1-z^{-1}}{T_o}\right)H_y + z^{-1}T_{Iy} \quad (24)$$

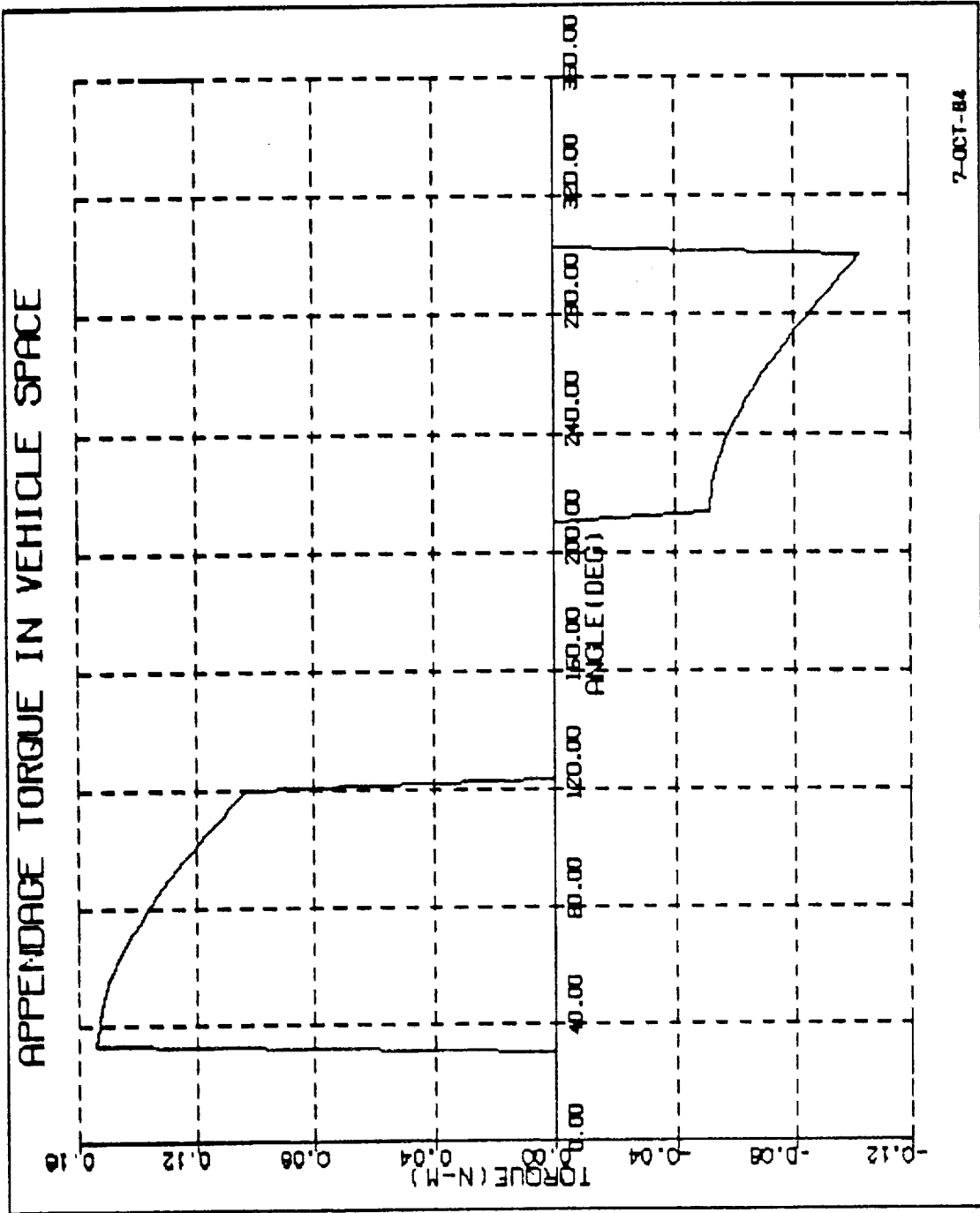
$$T_{Iy} = -\frac{\bar{H}_y}{T_o} - \frac{.5(1-z^{-1})H_y}{T_o} \quad (25)$$

$$T_{Dy} = T_{By} + T_{Iy} \quad (26)$$

$$\gamma = \sin^{-1}\left(\frac{\rho_{est} \cdot T_{Dy}}{\rho_{nom} \cdot T_{nom}}\right) \quad (27)$$

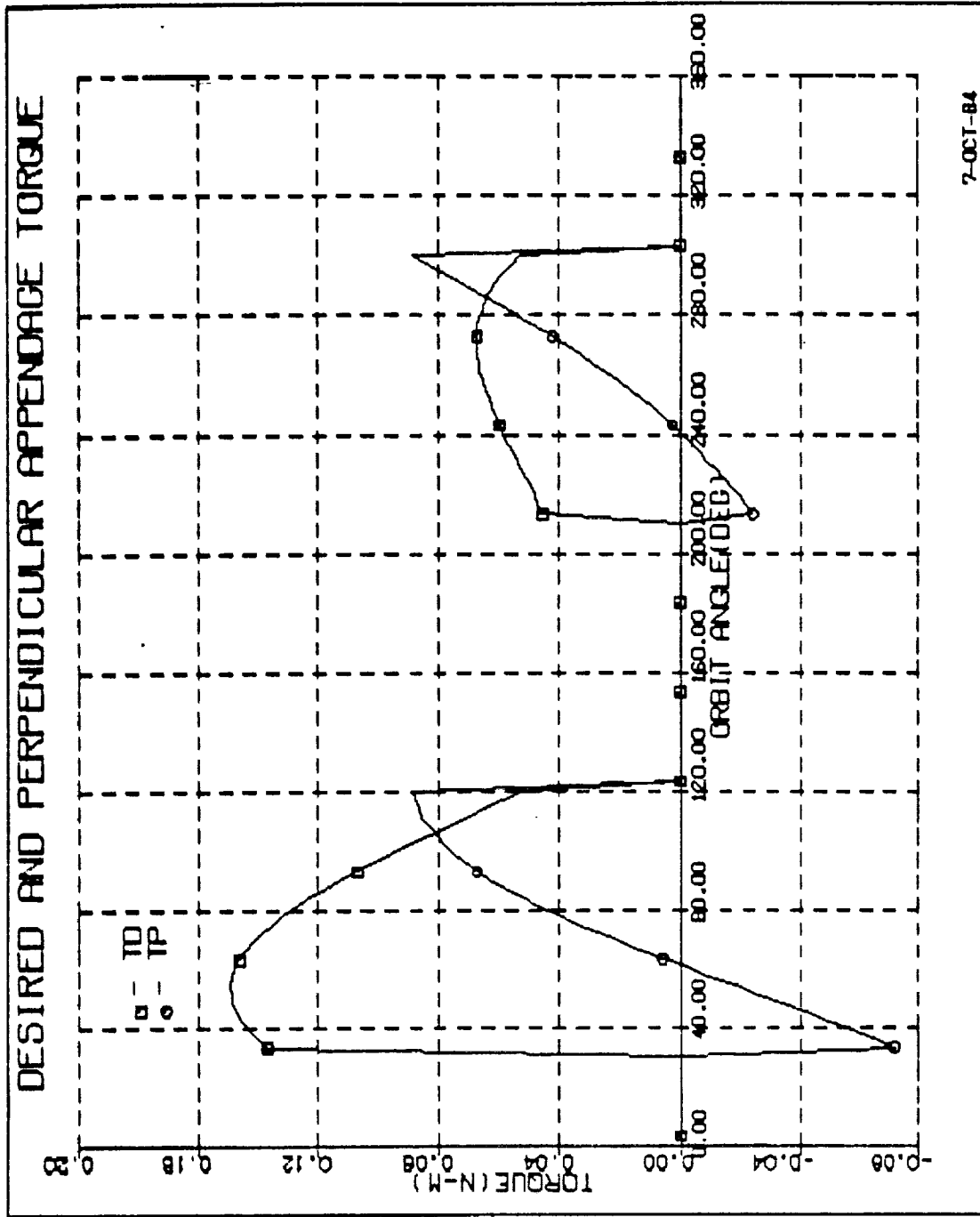
The sign of the desired torque determines which panel is "on". Figure 22 shows the IOP appendage torque in vehicle space for a typical orbit, Figure 23 shows the torque in the desired and perpendicular direction and Figure 24 shows the torque in OI axes. The torques shown are not perfect as they represent the torques generated by the control law using the first momentum samples. The closed loop nature of the calculations will assure that after every several orbits, the profile converges to produce the torque in the desired direction despite the non uniformity of the atmosphere. This non uniformity can be seen in Figure 22 where a constant ρ would produce a square wave profile.

Figures 25, 26 and 27 show IOP momentum buildup for nominal, 20% nominal and 5 times nominal average density over 9 orbits without bias counteraction. Figures 28, 29 and 30 show IOP momentum when the average density, nominal, 20% nominal and 5 times nominal, used in the control law exactly



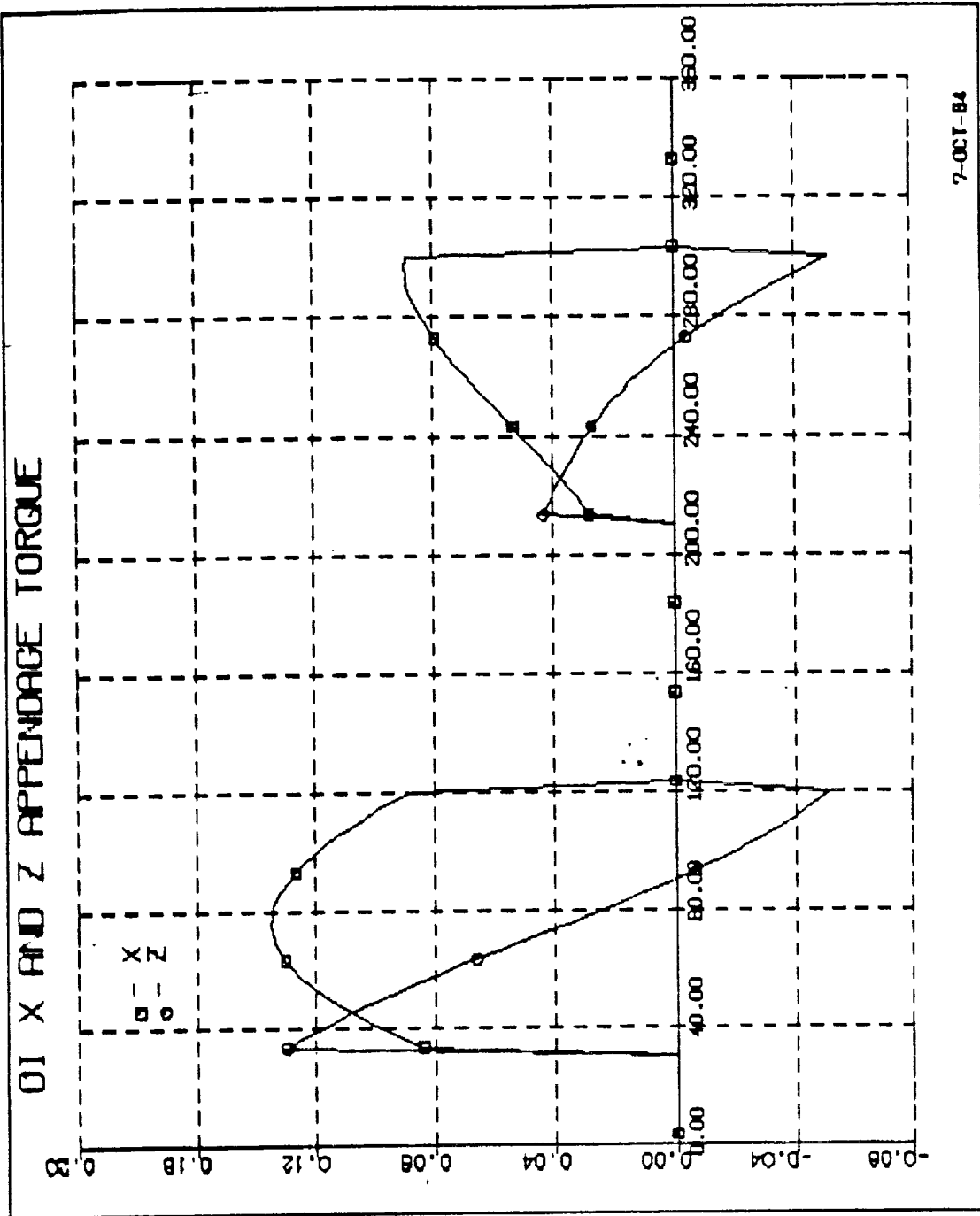
7-OCT-84

FIGURE 22 IOP APPENDAGE TORQUE IN VEHICLE SPACE



7-OCT-84

FIGURE 23 DESIRED AND PERPENDICULAR IOP APPENDAGE TORQUE



7-OCT-84

FIGURE 24 OI X AND Z APPENDAGE TORQUE

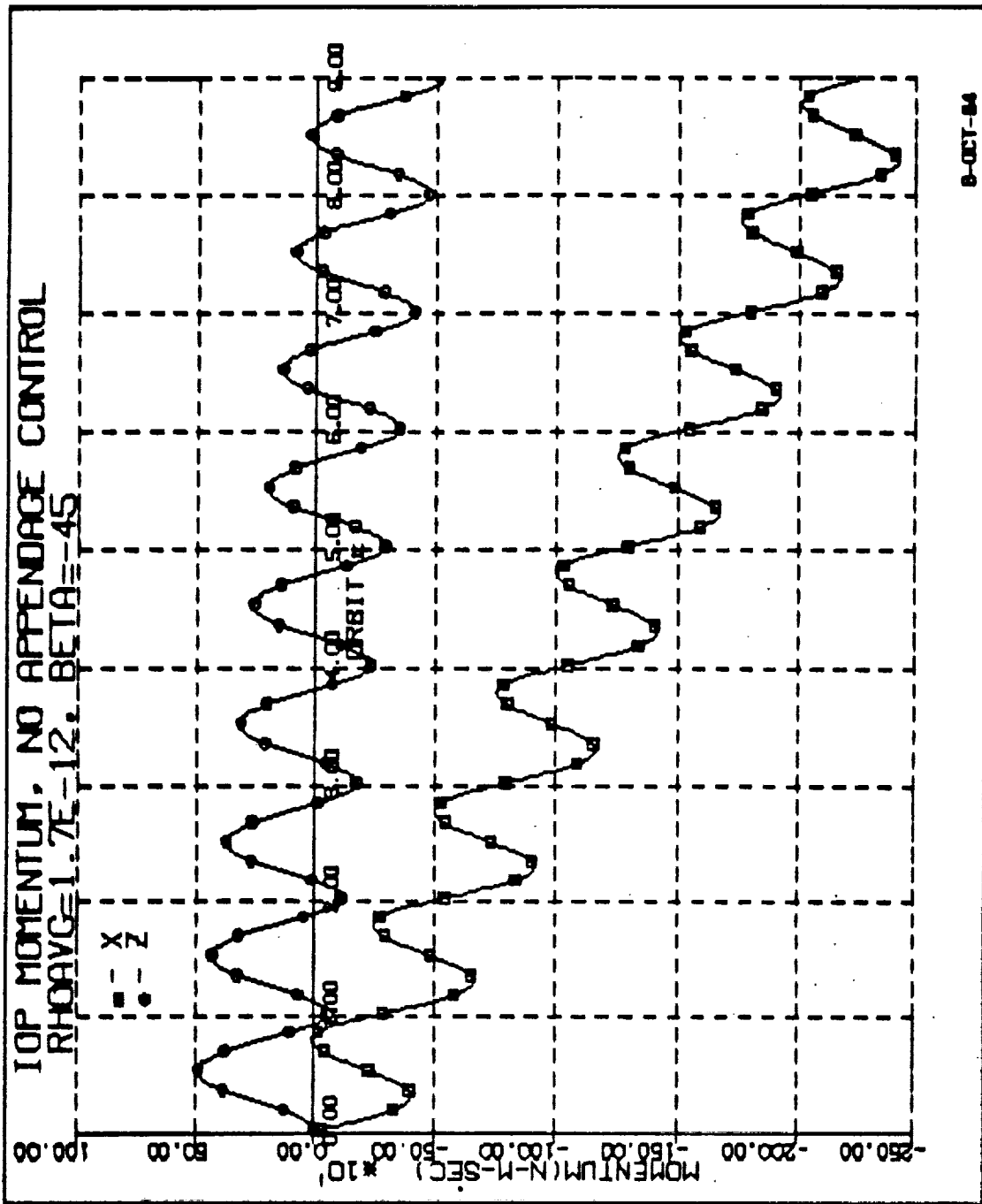


FIGURE 25
 IOP MOMENTUM, NO APPENDAGE CONTROL, RHOAVG = 1.7E-12, BETA = -45

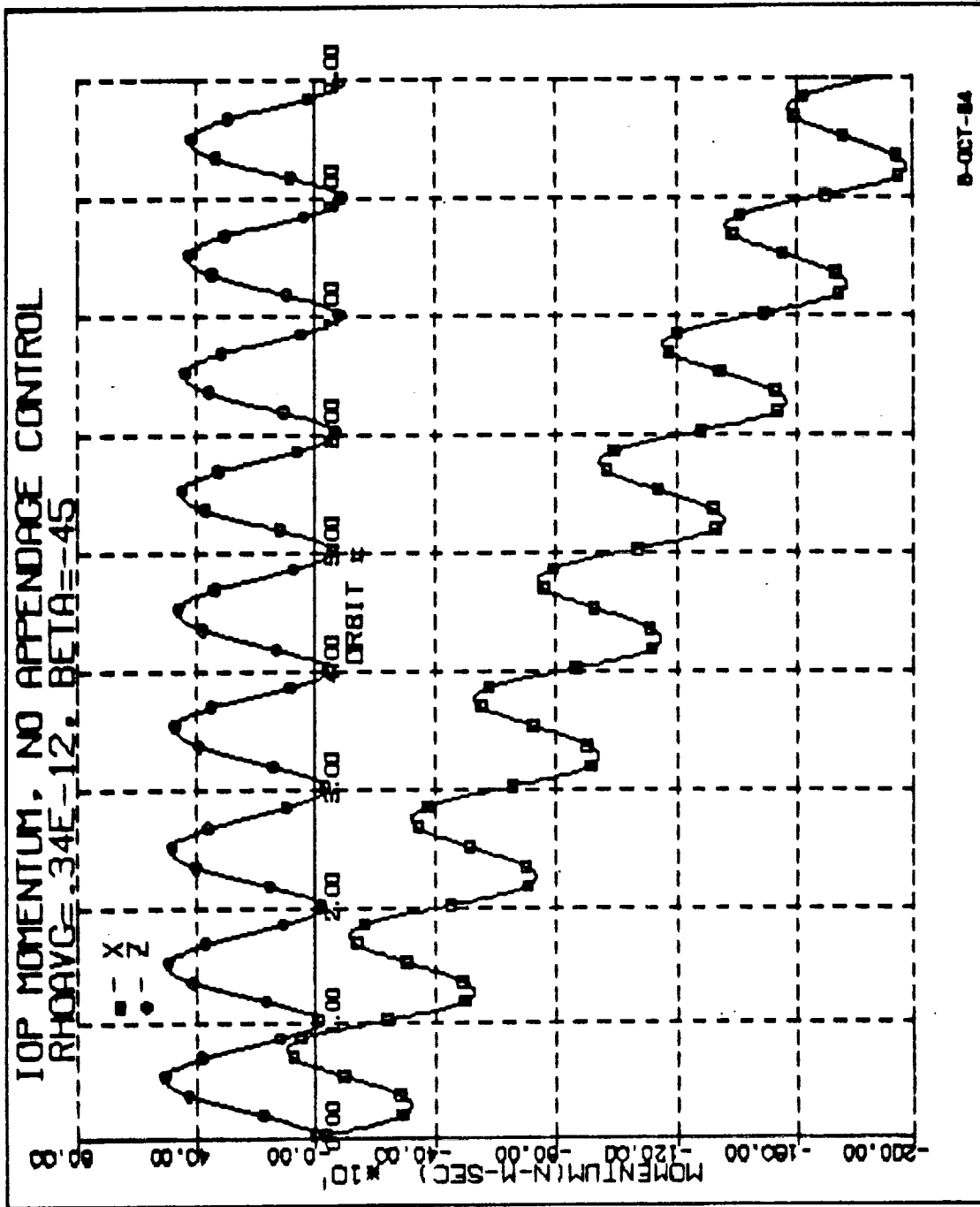


FIGURE 26
IOP MOMENTUM, NO APPENDAGE CONTROL, RHOAVG = .34E-12, BETA = -45

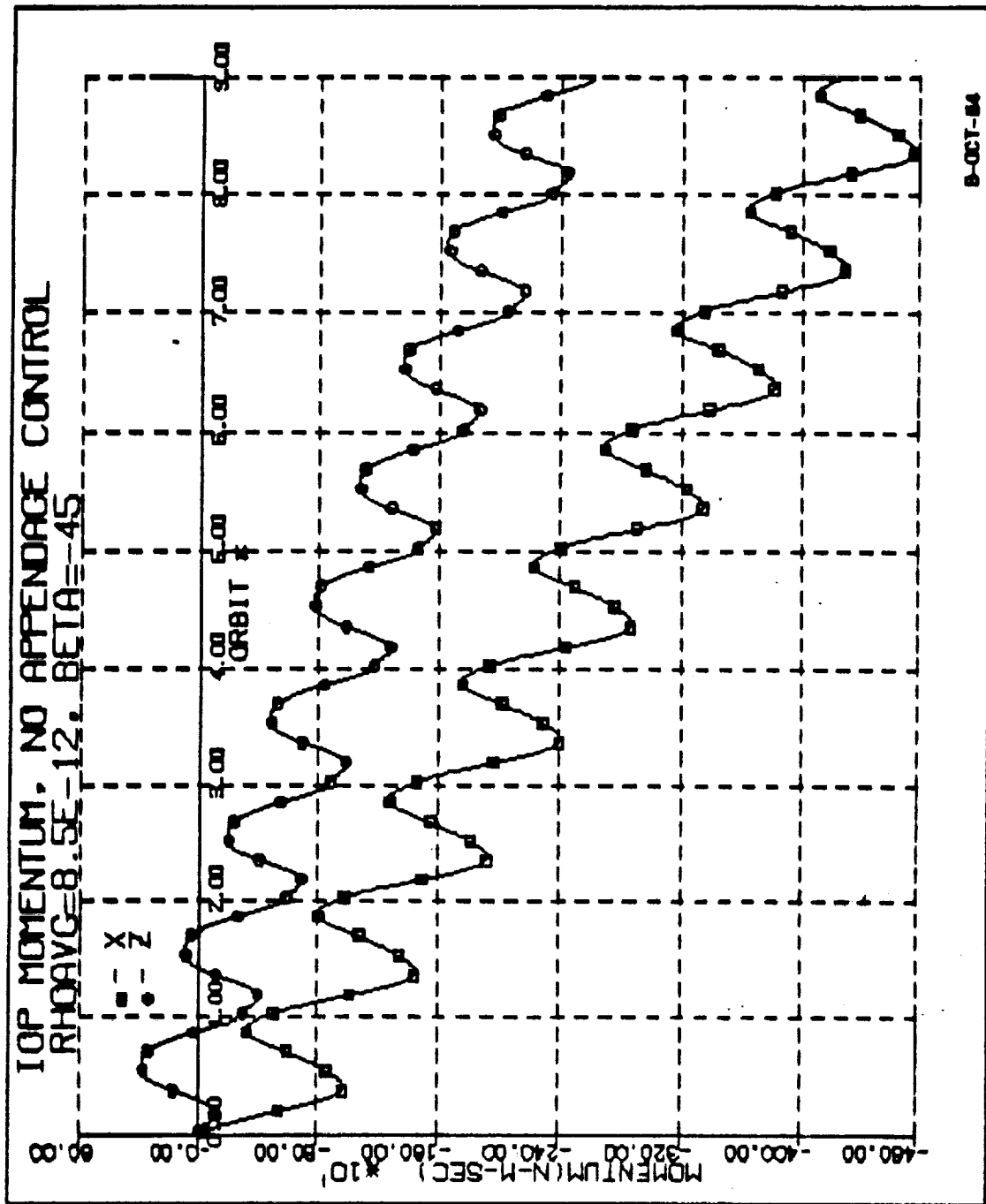


FIGURE 27

IOP MOMENTUM, NO APPENDAGE CONTROL, RHOAVG = 8.5E-12, BETA = -45

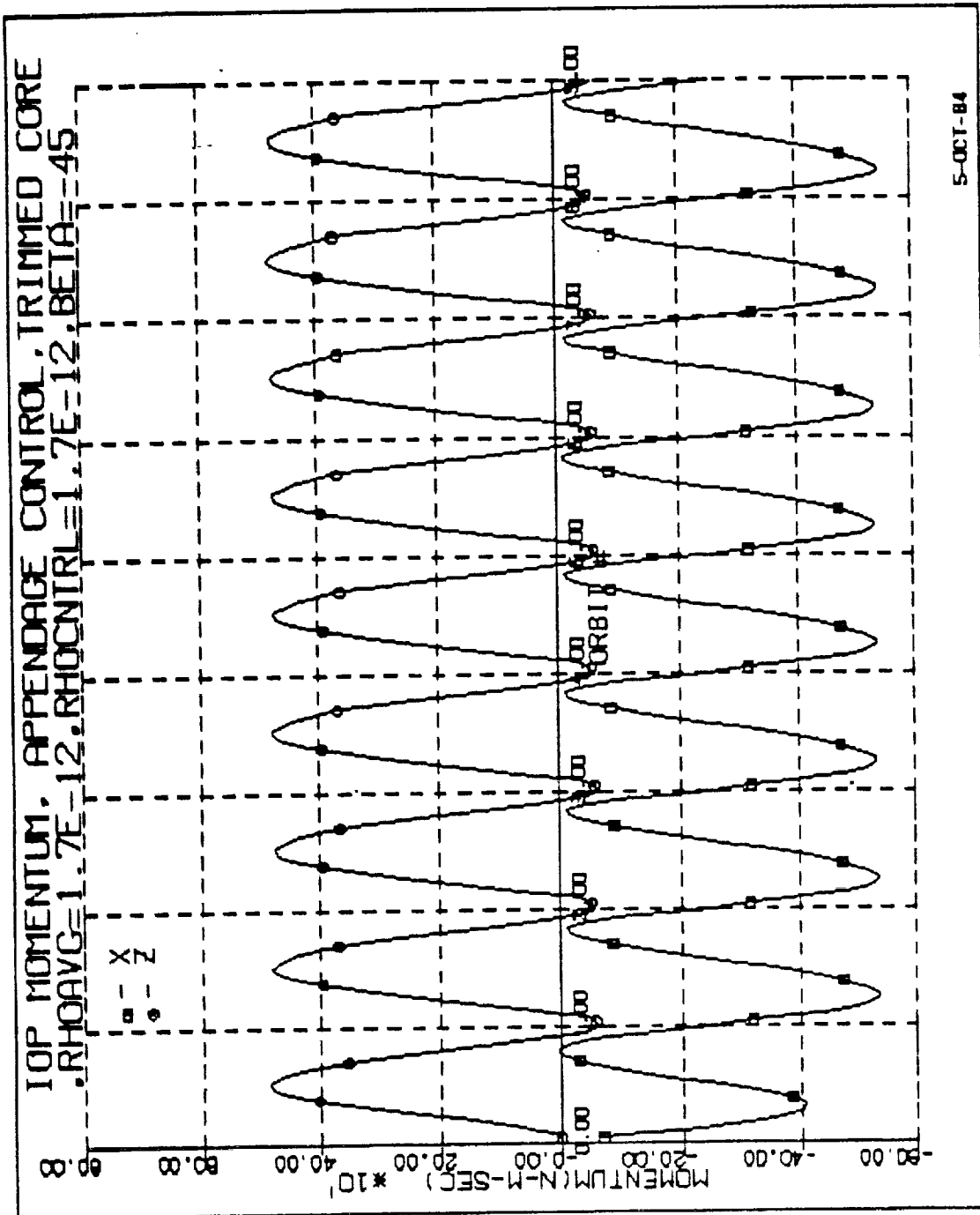


FIGURE 28
 IOP MOMENTUM, APPENDAGE CONTROL, TRIMMED CORE,
 RHOAVG = 1.7E-12, RHOCTRL = 1.7E-12, BETA = -45

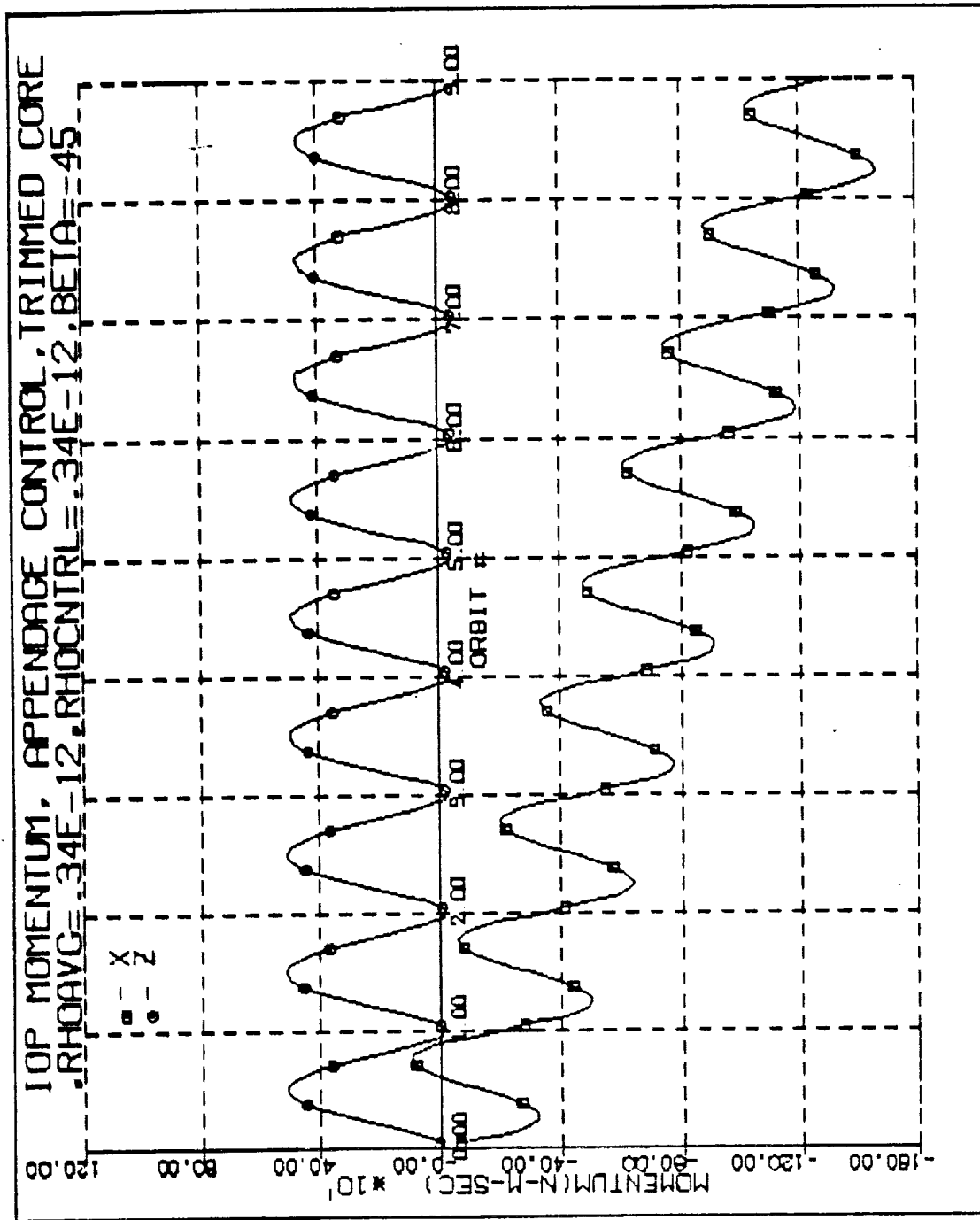


FIGURE 29
 IOP MOMENTUM, APPENDAGE CONTROL, TRIMMED CORE,
 RHOAVG = .34E-12, RHOCTRL = .34E-12, BETA = -45

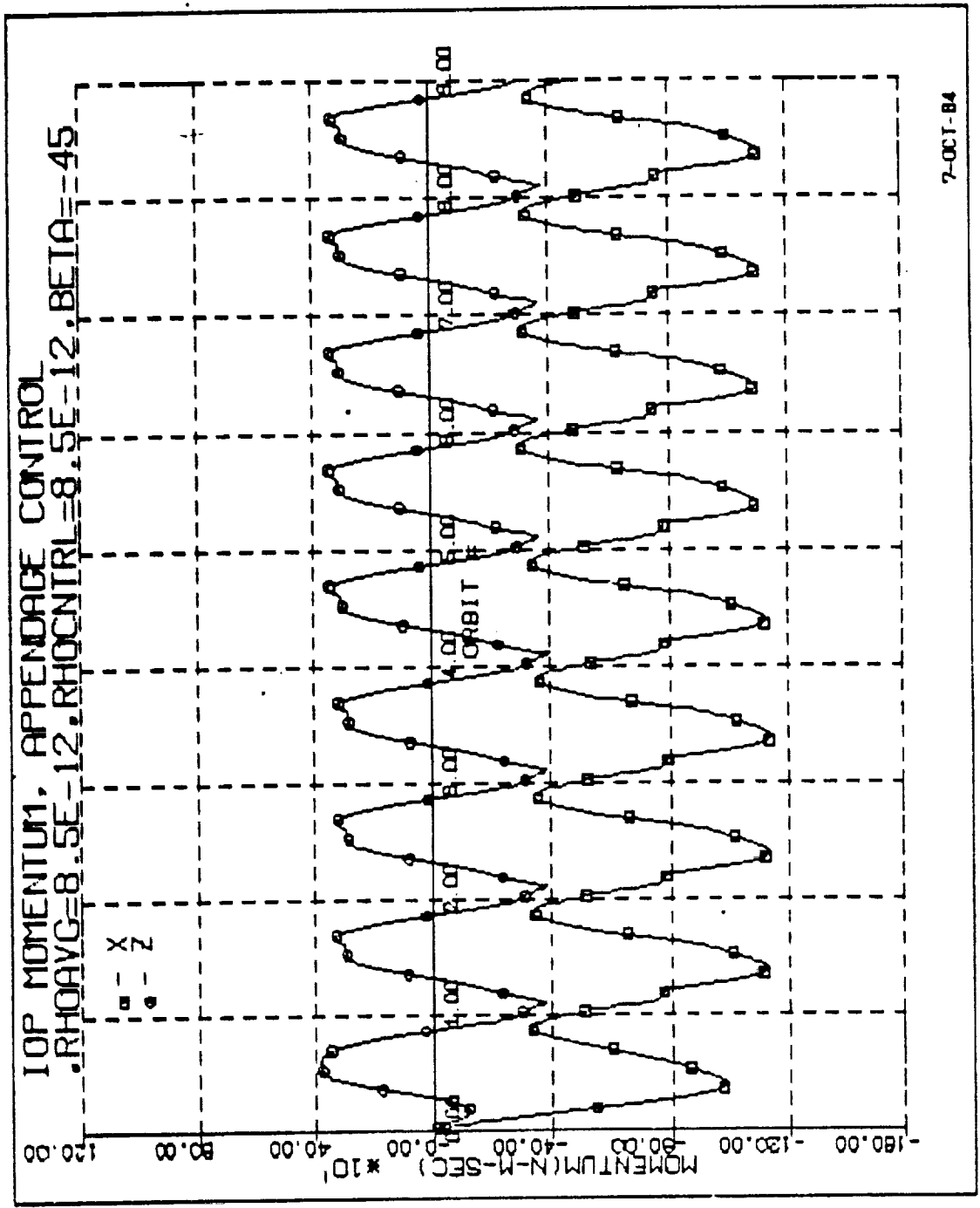


FIGURE 30
IOP MOMENTUM, APPENDAGE CONTROL, TRIMMED CORE,
RHOAVG = 8.5E-12, RHOCTRL = 8.5E-12, BETA = -45

matches the average atmospheric density. At the β -angle of -45 degrees, Figure 29 shows that regardless of the control law, the appendages can not counteract the IOP bias about the OI X-axis bias torque when the atmospheric density is only 20% nominal. The only solutions are to increase the panel size or raise the solar arrays for 0 degree β -angle as shown in Figure 31. This would reduce the available power if the actual β -angle were -45 degrees. Figure 32 shows IOP momentum when the ρ_{est} assumed by the control law is different from the true ρ_{avg} . The true density is 5 times that used by the control law and makes the IOP bias desaturation marginally stable.

The performance of the panels for POP desaturation is heavily dependent on the approximate balance of the vehicle gravity gradient and aerodynamic bias torques. Figure 33 shows the approximate POP axis trim as a function of ρ_{avg} where vehicle trim is the angle between the vehicle Z-axis and the local vertical. Figure 34 shows the POP appendage torque when one is perpendicular to the air flow and with the nominal atmospheric model. The appendages are capable of generating .1 N-m torque at the nominal ρ_{avg} which represents trim capability over one degree. At 5 times the nominal density, the trim capability is 5 degrees while at 20% the trim capability is only .2 degrees of vehicle attitude. Therefore reaching an approximately balanced attitude about the POP axis using gravity gradient desaturation is most critical during periods low atmospheric density. Figures 35, 36 and 37 show the POP momentum for an approximately trimmed vehicle at nominal, 20% nominal and 5 times nominal density without additional appendage desaturation. Approximately trimmed means the the POP bias is not perfectly balanced but within the capability of the aerodynamic desaturation panels when the density in the control law is exactly matched to the average density. Figures 38, 39 and 40 show typical POP momentum where the vehicle is trimmed and the true density and that assumed in the control law are matched. Figure 41 shows the POP momentum when the true ρ_{avg} is 5 times that assumed by the control law. Only a slight oscillation can be seen so that POP desaturation is quite insensitive to a ρ_{avg} greater than that assumed by the control law. However if the ρ_{avg} is less than that assumed by the control law, the degree of core body trim might be inadequate and the POP momentum would diverge. The divergence is not caused by lack of robustness in the controller but by insufficient torque capability.

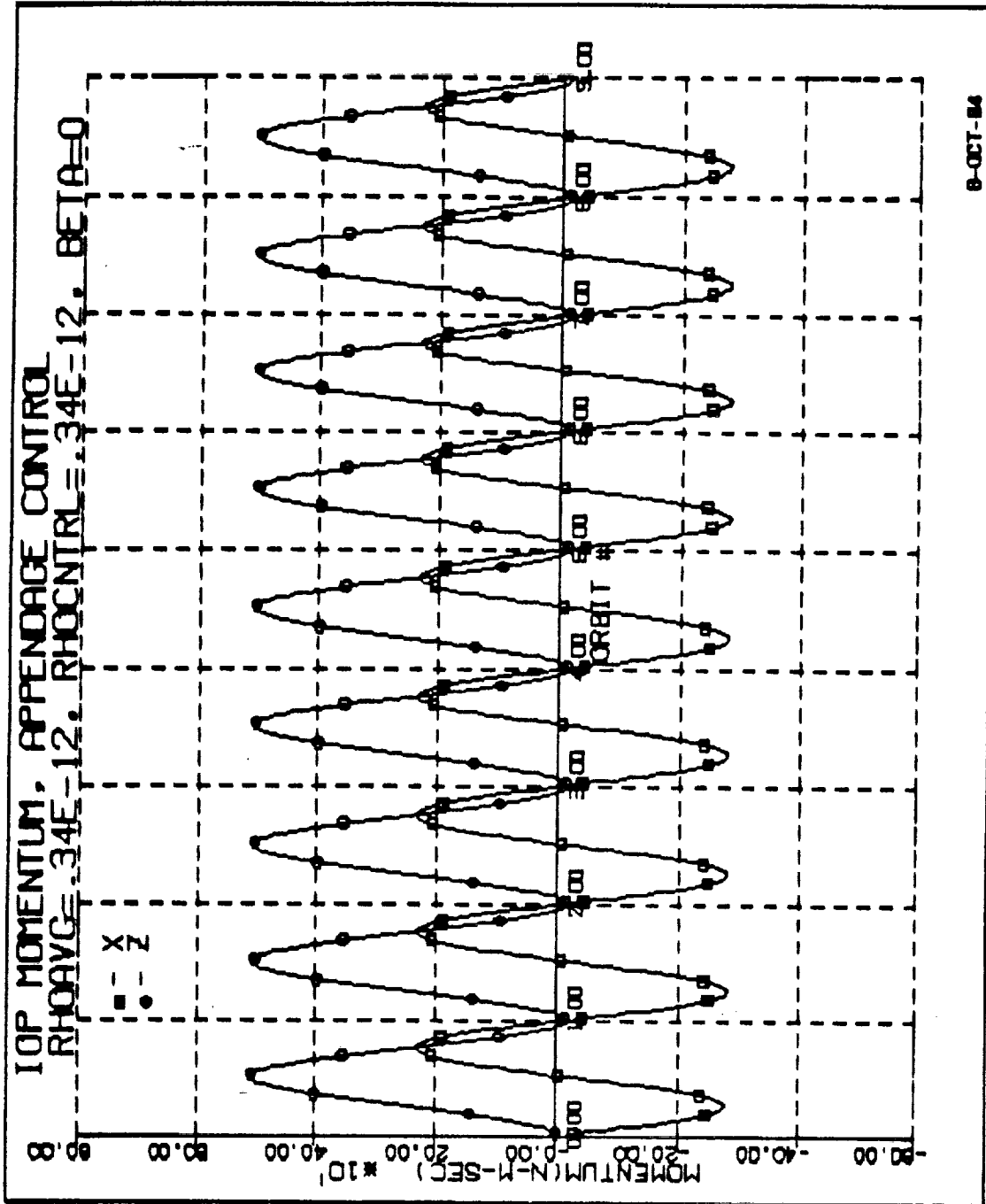


FIGURE 31
 IOP MOMENTUM, APPENDAGE CONTROL, TRIMMED CORE,
 $\text{RHOAVG} = .34\text{-}12$, $\text{RHOCTRL} = .34\text{-}12$, $\text{BETA} = 0$

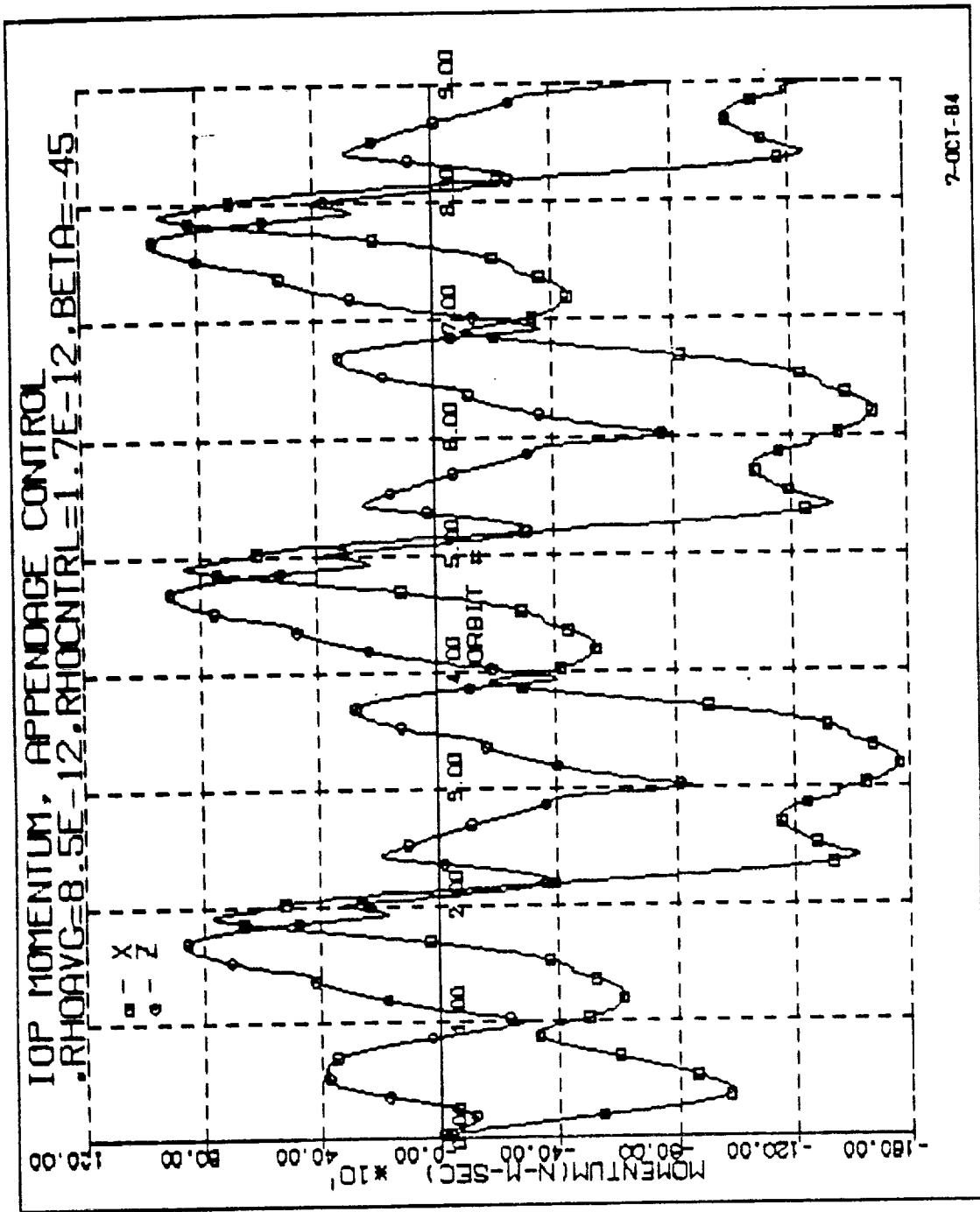


FIGURE 32
 IOP MOMENTUM, APPENDAGE CONTROL,
 RHOAVG = 8.5E-12, RHOCTRL = 1.7E-12, BETA = -45

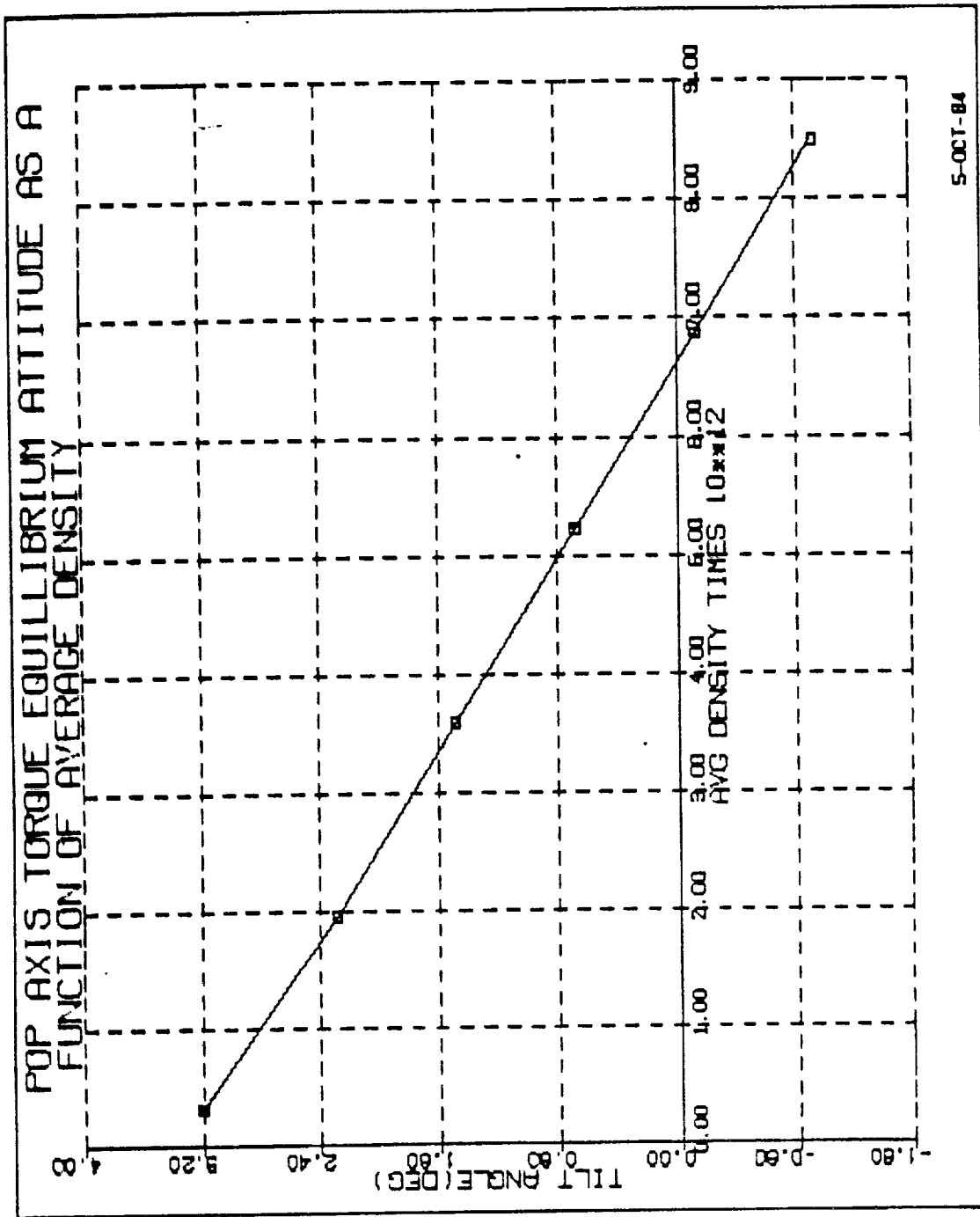


FIGURE 33
POP AXIS TORQUE EQUILIBRIUM ATTITUDE AS A FUNCTION OF AVERAGE DENSITY

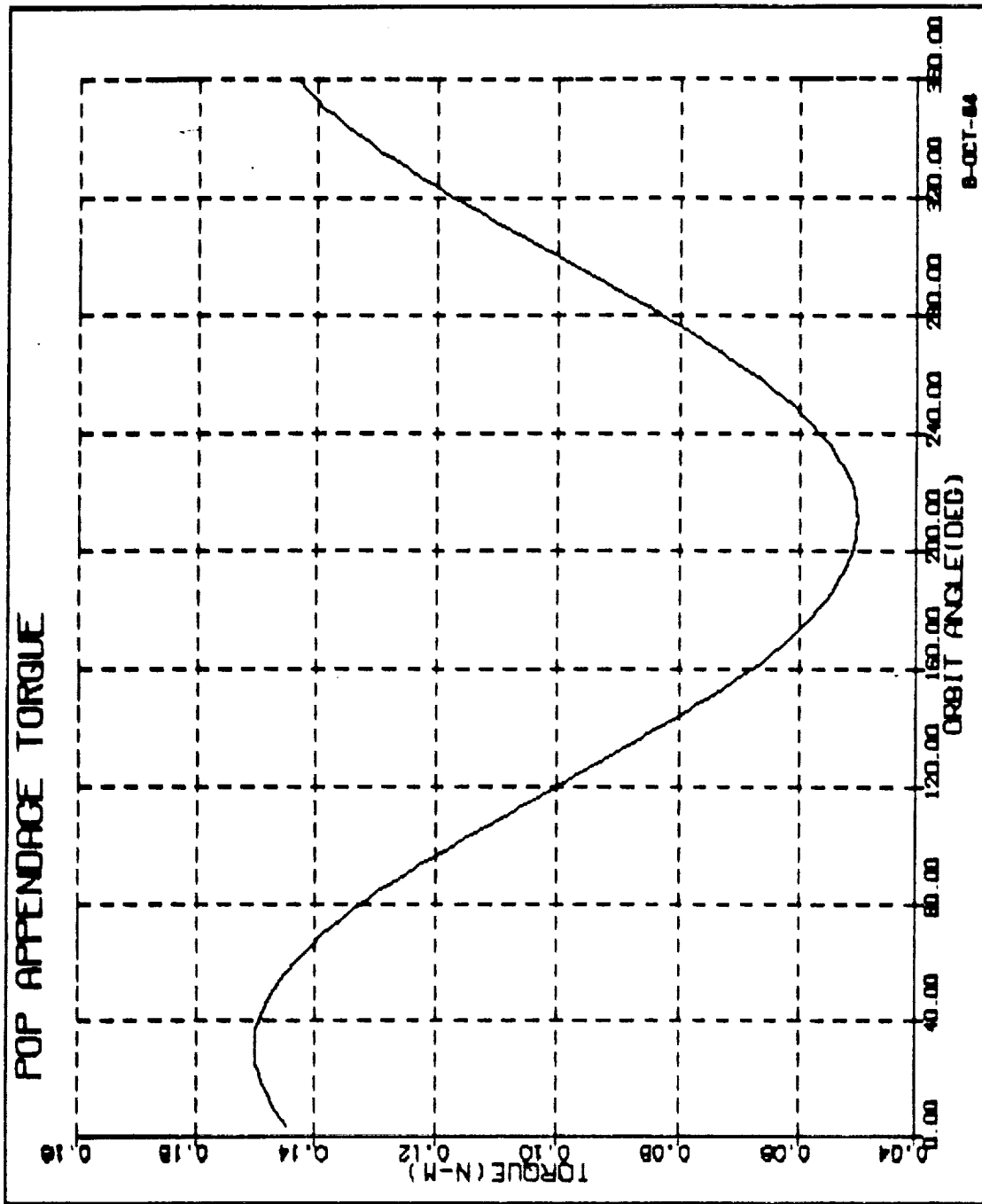


FIGURE 34 POP APPENDAGE TORQUE

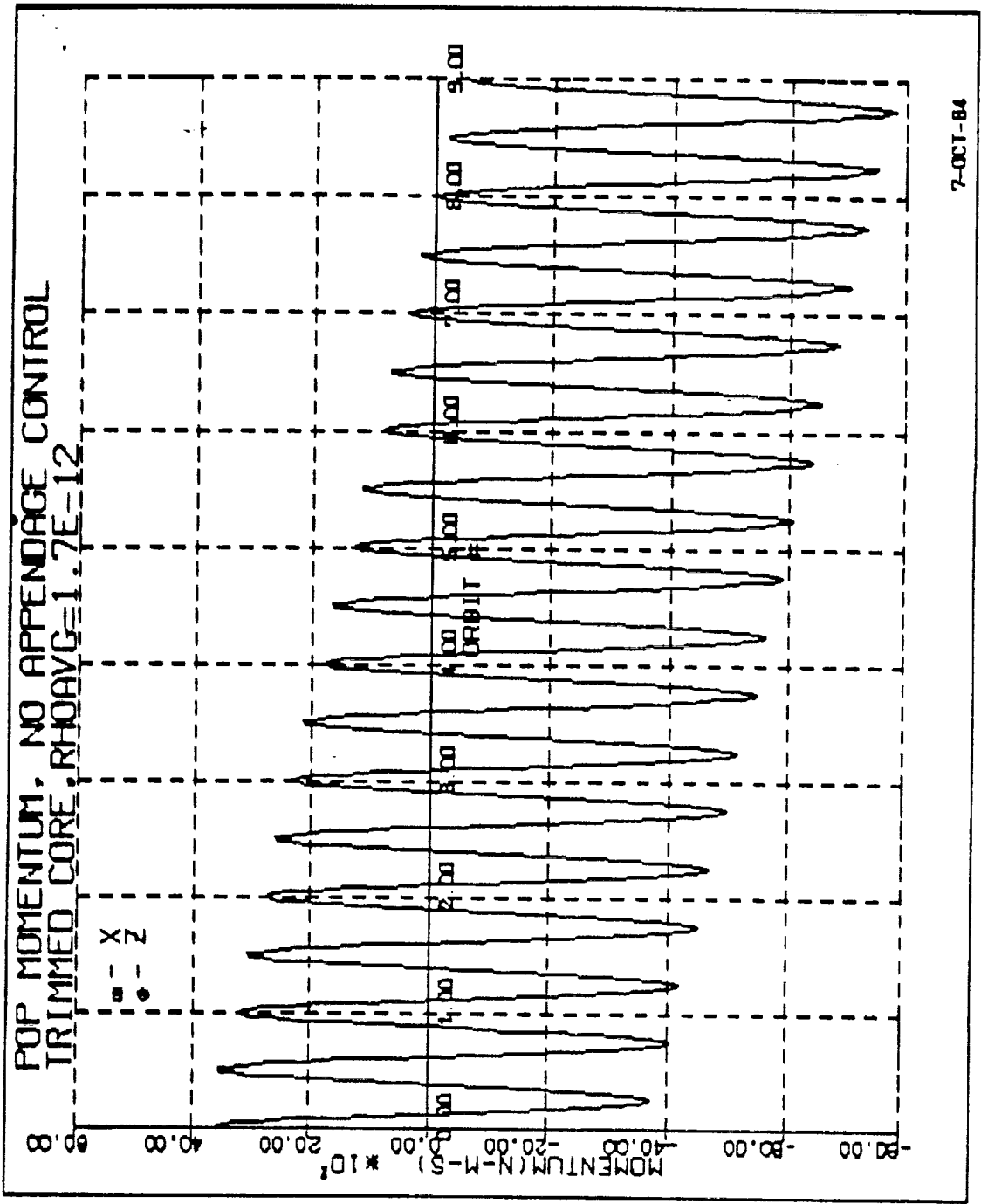


FIGURE 35

POP MOMENTUM, NO APPENDAGE CONTROL, TRIMMED CORE, RHOAVG = 1.7E-12

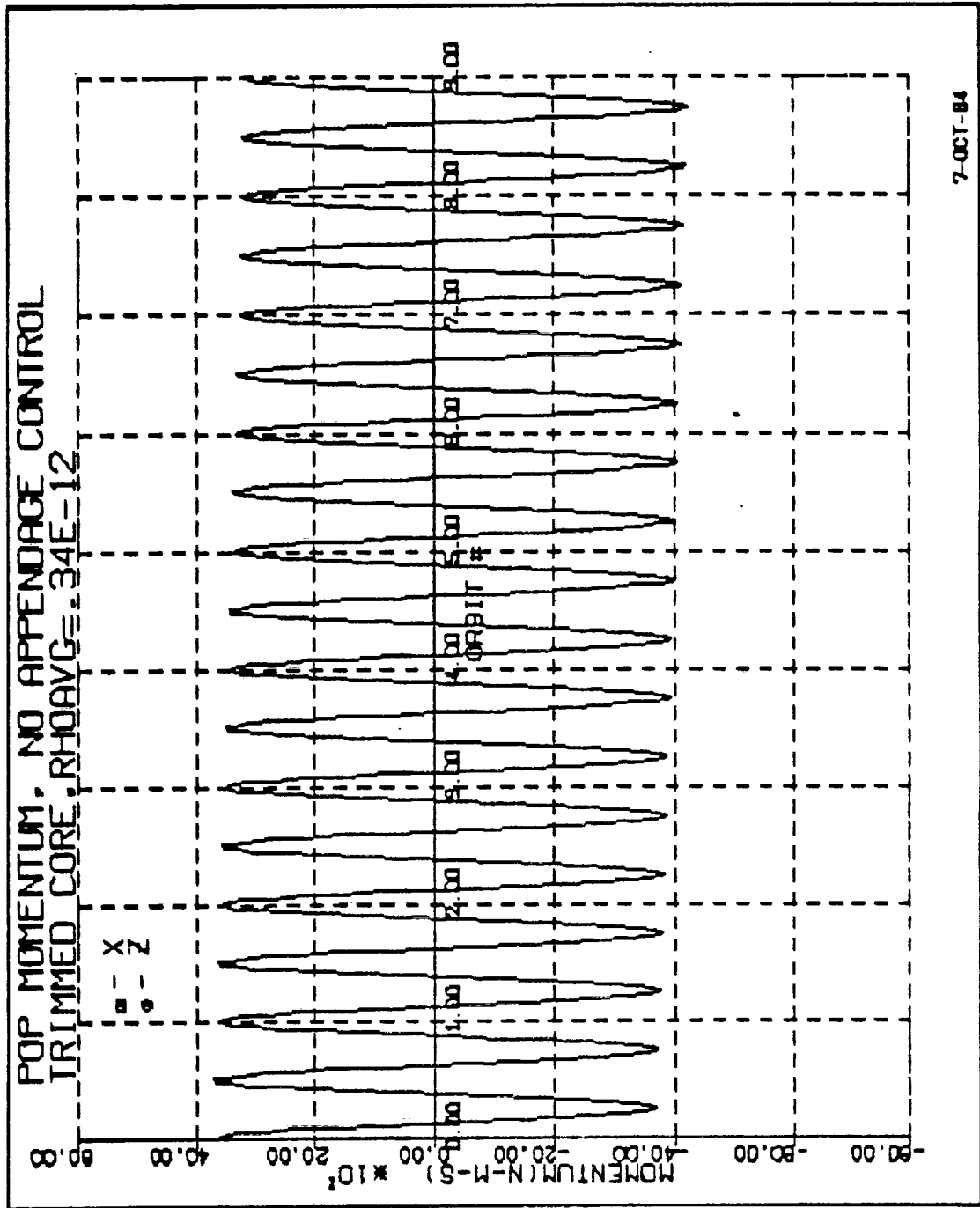


FIGURE 36
POP MOMENTUM, NO APPENDAGE CONTROL, TRIMMED CORE,
RHOAVG = .34E-12, RHOCTRL = .34E-12, BETA = -45

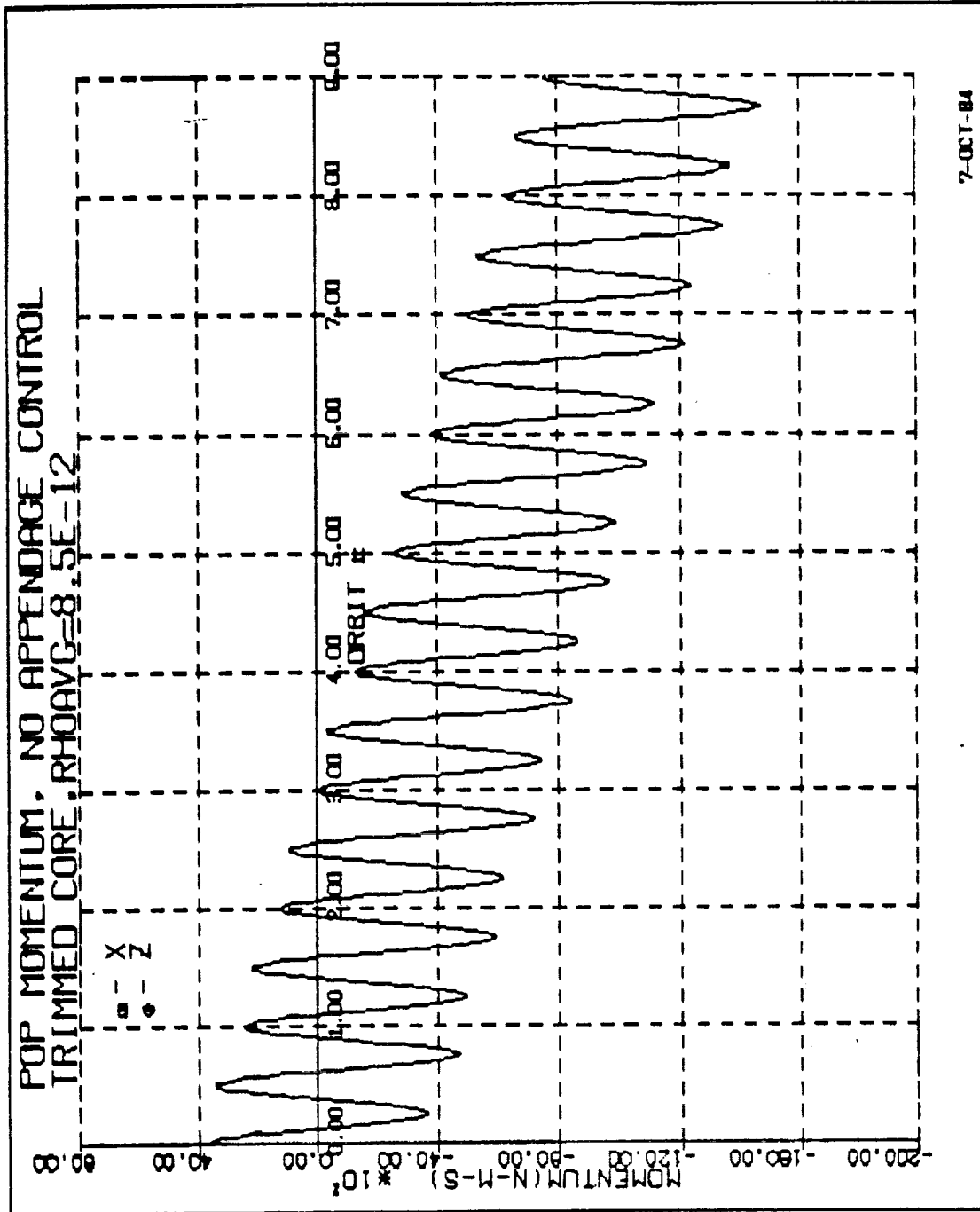


FIGURE 37
 POP MOMENTUM, NO APPENDAGE CONTROL, TRIMMED CORE, RHOAVG = 1.7E-12

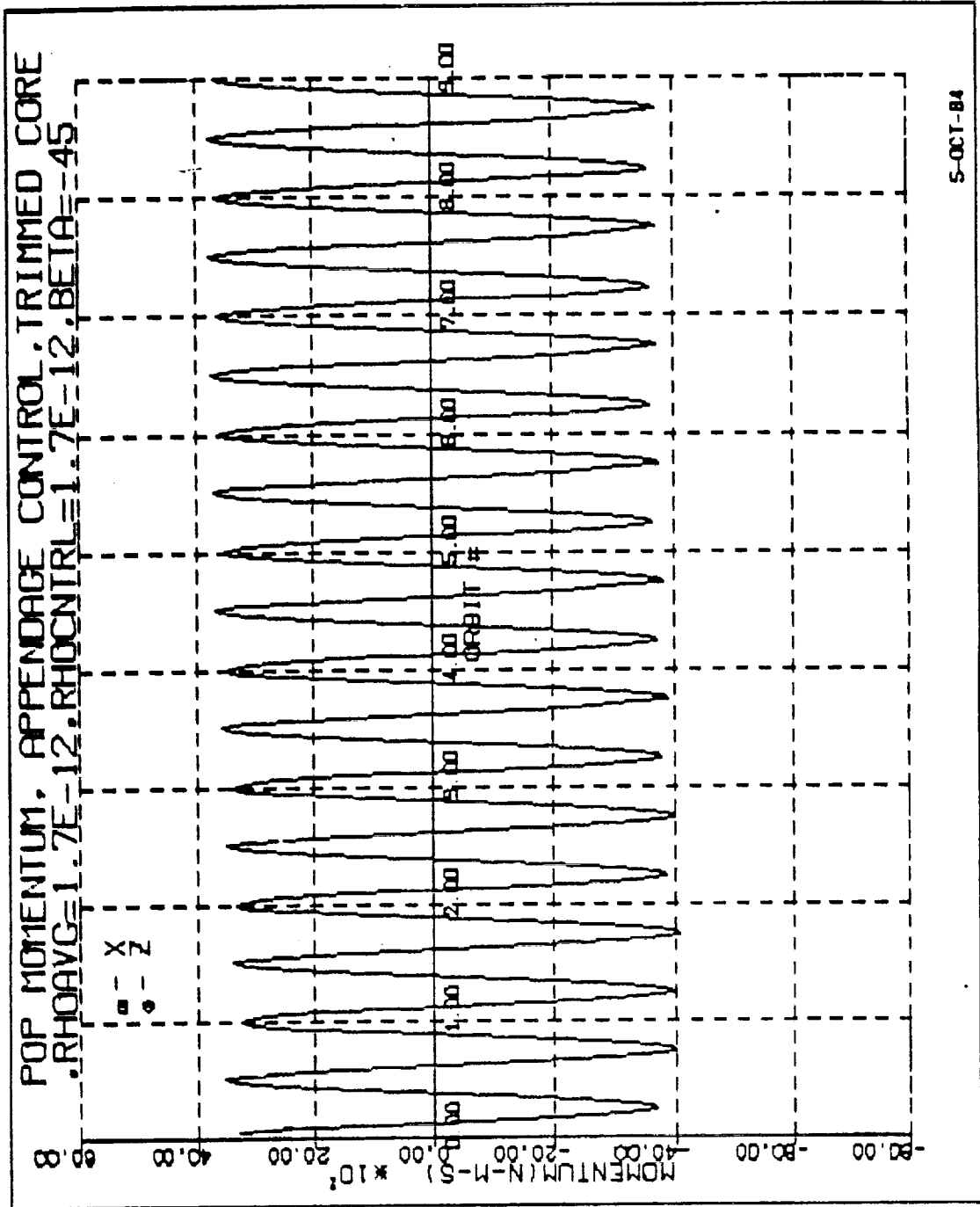


FIGURE 38
 POP MOMENTUM, APPENDAGE CONTROL, TRIMMED CORE,
 RHOAVG = 1.7E-12, RHOCTRL = 1.7E-12, BETA = -45

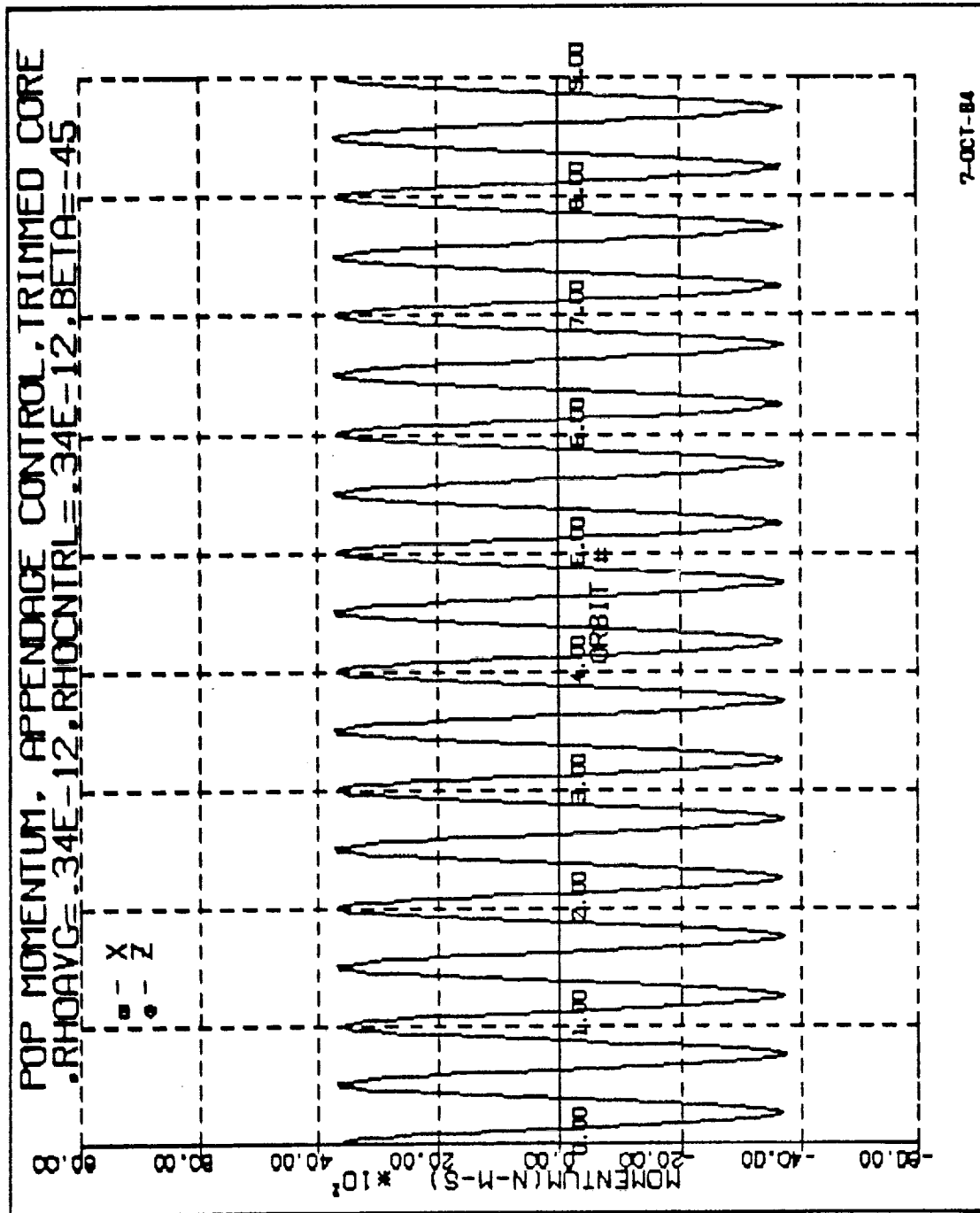


FIGURE 39
 POP MOMENTUM, APPENDAGE CONTROL, TRIMMED CORE, RHOAVG = .34E-12

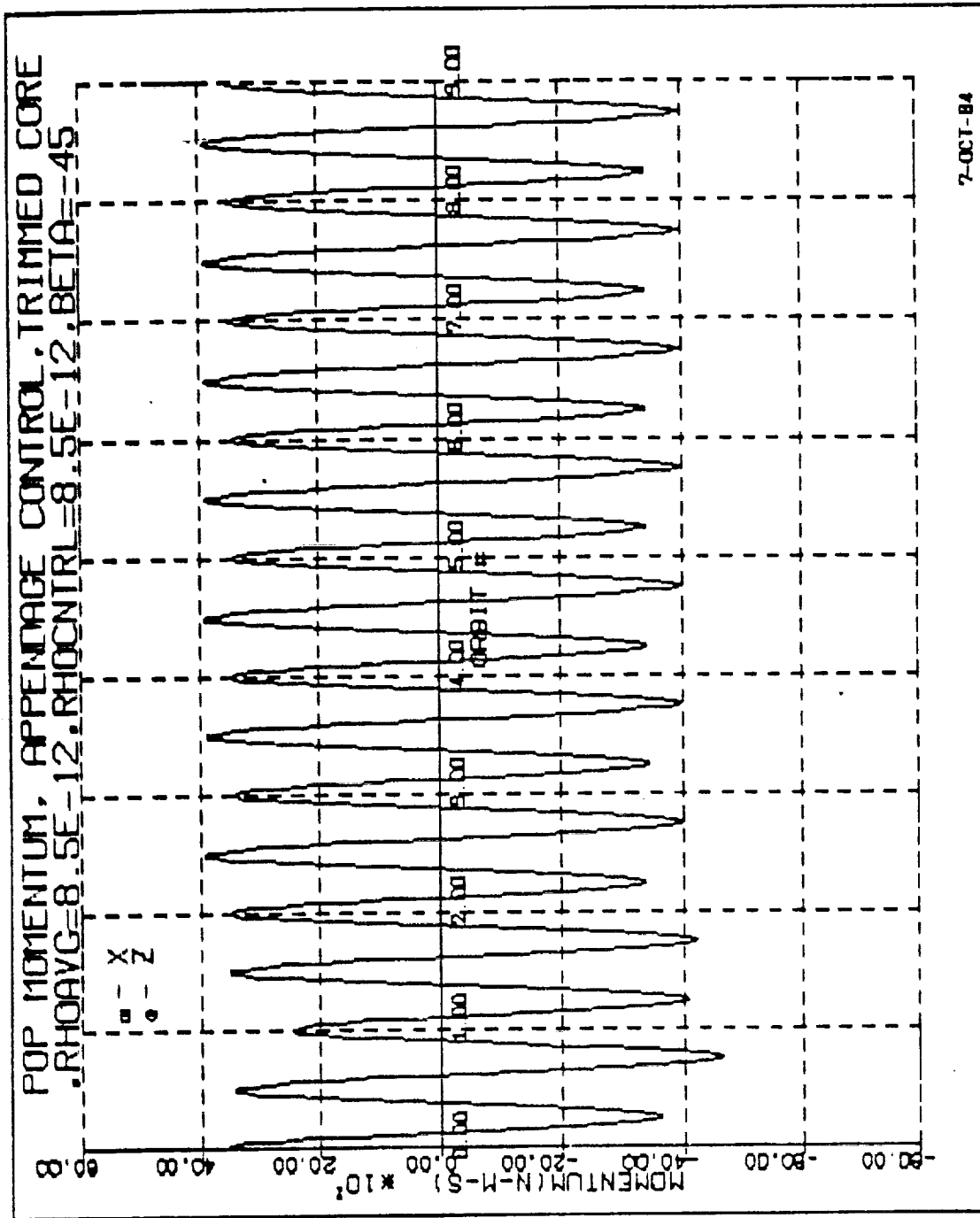


FIGURE 40
 IOP MOMENTUM, APPENDAGE CONTROL, TRIMMED CORE,
 RHOAVG = 8.5E-12, RHOCTRL = 8.5E-12, BETA = -45

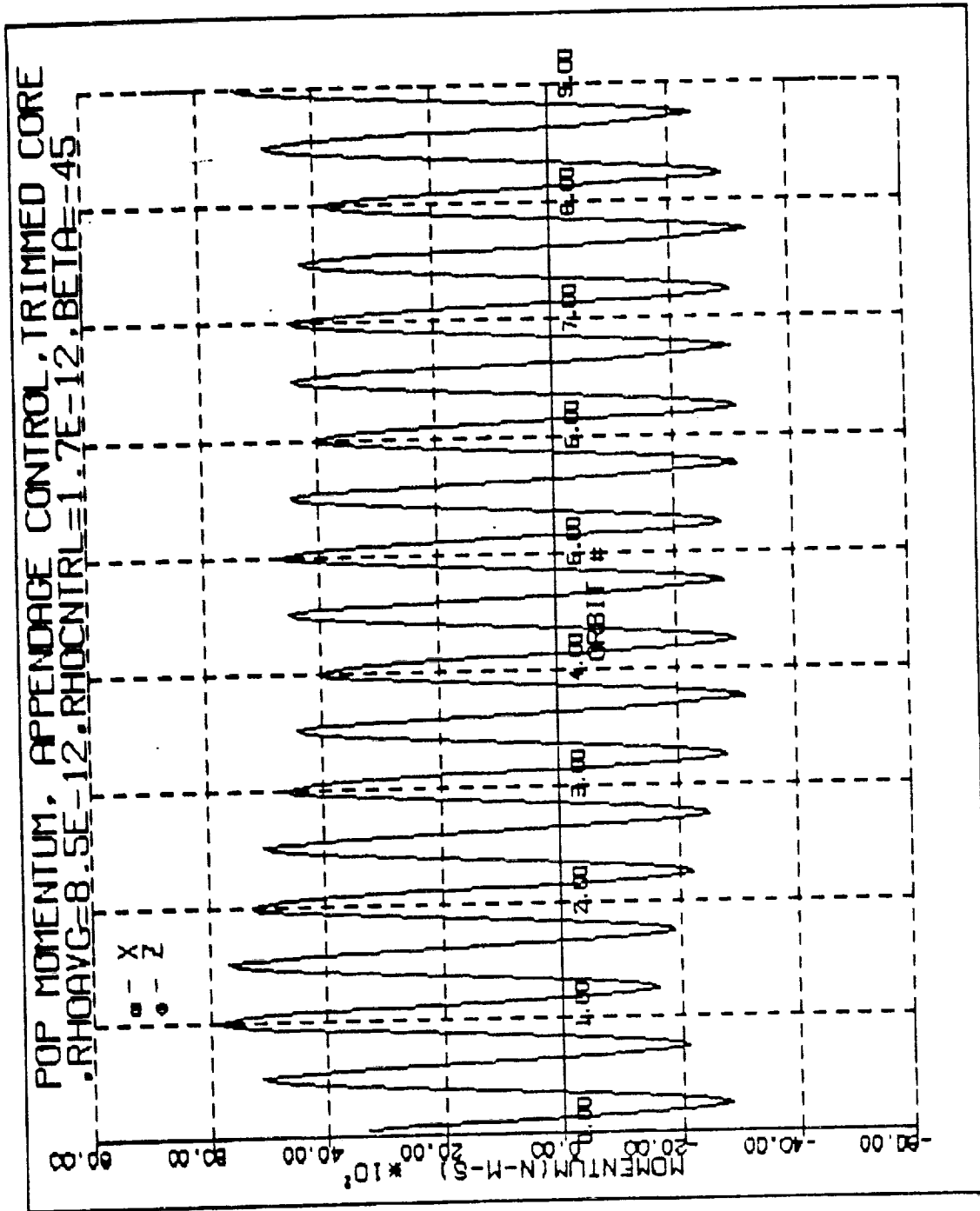


FIGURE 41
 POP MOMENTUM, APPENDAGE CONTROL, TRIMMED CORE,
 RHOAVG = 8.5E-12, RHOCTRL = 1.7E-12, BETA = -45

6.0 Conclusions and Recommendations

Two viable new techniques of momentum management for the the CDG Planar Space Station configuration have been developed. These are the use of the core body for gravity gradient desaturation and the implementation of four flat plate appendages at the end of long booms which would be used for aerodynamic desaturation. The use of the core body, whose attitude is nominally local vertical, for gravity gradient desaturation about the POP direction is a technique previously considered. The control law developed in this study shows that the core body can also be used to autonomously center POP momentum therefore minimizing momentum storage requirements.

Using the core body to desaturate momentum IOP required a phased rotation about the vehicle X-axis to generated torque IOP with the desired magnitude and direction. All calculations using the core body for desaturation were autonomous and required only knowledge of the core body inertia matrix. With the exception of momentum sampling, calculations were only performed at orbital frequency and should impose very little burden on a flight computer. Examination of the results showed that after equilibrium was attained, only small core body rotations at orbital frequency were required to control the momentum.

As even these small rotations could interfere with payload pointing, an alternative method of momentum management using the core was developed. This method allowed the absolute momentum stored by the CMGs for an approximately trimmed vehicle to slowly drift to a value inside the maximum storage sphere of four Skylab type CMGs. At that time, the control law would initiate a maneuver, using the remaining CMG momentum, to remove the POP bias and re-center the POP momentum. The law would drive the IOP momentum along a diagonal to the opposite value of the IOP momentum circle. For these larger maneuvers, the profile was adjusted for finite vehicle maneuvering capability. This concept worked extremely well as maneuvers were required only about every thirtieth orbit. However the simulation did not include time varying external parameters such as β -angles and density functions.

To allow a trimmed vehicle to retain an inertial attitude for even longer periods of time, the aerodynamic desaturation appendages considered could be used. They do represent additional hardware requirements but an examination of the results shows that the method is competitive with the benchmark, magnetic desaturation. The total weight would probably be less than the 170kg of the Space Telescope magnetic desaturation system and the power required much less than the 120 watts required at maximum magnetic moment. However the control law utilizing these appendages does require at least an approximate value of the average air density during an orbit. Doubt exists as to the availability of this parameter but the control law developed has been shown to be relatively insensitive to atmospheric density uncertainties. One possibility is to autonomously obtain an estimate of ρ_{avg} from the POP axis trim angle.

During periods of high atmospheric density, appendage desaturation is capable of much larger torques than four Space Telescope torquer bars. During periods of very low atmospheric density, a higher degree of attitude trim might be required for the POP axis. IOP desaturation could be difficult since the appendages do not generate sufficient torque to counteract solar array GG bias torques at 45 degree β -angle. Appendages do not present the problems of magnetic contamination of payloads but potential problems could exist with line-of-sight of payloads and attitude control position sensors. Due to the light weight and stiff construction proposed (Kevlar Boom), no attitude control structural mode induced control problems are anticipated and the transmission of torques to the core body should be quite rigid. By means of transformations stored in the attitude control computer, magnetic desaturation performs independently of vehicle attitude since a magnetic moment can be defined in orbit inertial space. The appendage control law defined in this study only operates at the CDG Planar Space Station baseline attitude. Should appendage desaturation be desired at a variety of attitudes, the modified concepts could still be feasible but the appendages would require at least two-degrees-of-freedom. Additional studies could define the appendage/boom/actuator systems in greater detail and also evaluate control law performance over changing β -angles and atmospheric densities.

7.0 References

Wertz, James R. (Editor) Spacecraft Attitude Determination and Control, D. Reidel Publishing Co., 1978.

Barrows, D., Bedell, H., Hahn, E., Kaczynski, R., Levinthal, J. Momentum Management for the Space Platform, American Astronautical Society, AAS 82-004, 1982.

Kaczynski, R. F., Momentum Management Utilizing Gravity Gradient Torquing, Bendix GSD Report MMS-83-1, Oct 1983.

Kaczynski, R. F. Spacecraft Aerodynamic Torques Due to an Inertially Oriented Flat Plate Area Bendix GSD Document No. 5460476-MT, April 1982.

Levinthal J., Morata, L., and Powell L., Space Platform Attitude Control System International Federation Automatic Control, Netherlands, 1982.

Hahn, E., Kaczynski, R., Barrows, D., Autonomous Momentum Management for the Space Platform AIAA-84-2006; AIAA/AAS Astrodynamics Conference, Seattle, 1984.

Nasa SP-8021, Models of Earth's Atmosphere, Revised March 1982.